Table 4. Continued

Affi ID	Gene abbreviation	Fold change CB 1	CB 2	PB 1	PB 2	Gene name
203329_at	*PTPRM*	0·36	0·62	1·38	1·93	Protein tyrosine phosphatase, receptor type, M
204731_at	*TGFBR3*	0·78	0·55	1·22	2·04	Transforming growth factor, beta receptor III (betaglycan, 300 kDa)
Transcription						
203129_s_at	*KIF5C*	0·67	0·09	1·33	3·43	Kinesin family member 5C
213906_at	*MYBL1*	0·75	0·51	1·25	3·63	V-myb myeloblastosis viral oncogene homologue (avian)-like 1
209815_at	*PTCH*	0·59	0·27	1·41	4·17	Patched homologue (*Drosophila*)
213891_s_at	*TCF4*	0·74	0·65	2·06	1·26	Transcription factor 4
238520_at	*TRERF1*	0·70	0·77	1·23	2·30	Transcriptional regulating factor 1
203603_s_at	*ZFHX1B*	0·74	0·61	1·26	3·63	Zinc finger homobox 1b
213218_at	*ZNF187*	0·74	0·69	1·26	1·76	Zinc finger protein 187
221123_x_at	*ZNF395*	0·38	0·71	1·63	1·29	Zinc finger protein 395

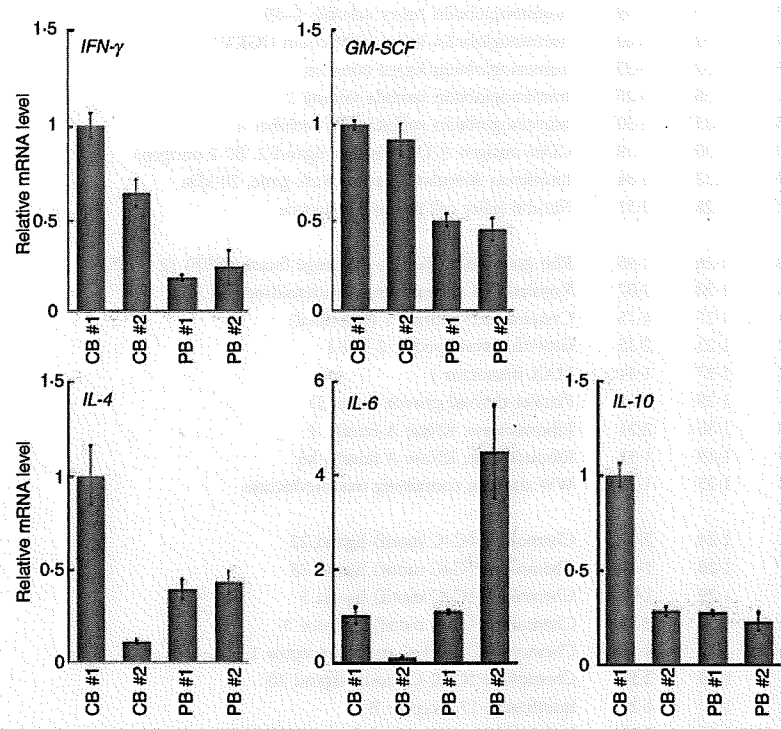

Figure 2. Quantitative polymerase chain reaction (PCR) analysis of the genes related to the T helper type 1 (Th1) and Th2 phenotypes. The expression of the genes indicated was examined by real-time reverse transcriptase (RT)-PCR using the same sample specimens as in Fig 1. Data are normalized to the mRNA level in PB 1 which is arbitrarily set to 1. The signal intensity was normalized using that of a control housekeeping gene [the human glyceraldehyde-3-phosphate dehydrogenase (*GAPDH*) gene]. Data are relative values with the standard deviation (SD) for triplicate wells.

significantly higher in PB-derived $CD4^+$ T cells in comparison with equivalent CB-derived $CD4^+$ T cells at 1 week ($P < 0·05$) but not at 2 weeks (Fig. 6).

Discussion

Although it is generally believed that there are functional differences between CB and PB lymphocytes, the details are obscure. For instance, Azuma *et al.*[13] reported that the phenotype and function of expanded CB lymphocytes were essentially equivalent to those of expanded PB lymphocytes when evaluated in *in vitro* experiments. In the present study, however, we have shown that CB-derived $CD4^+$ T cells revealed a distinct expression profile of genes important for the function of particular T-cell subsets compared with PB-derived $CD4^+$ T cells.

$CD4^+$ T cells can be classified into distinct subsets, including effector $CD4^+$ cells and Tregs, according to their functional characteristics as well as differentiation profiles.[14–16] Typically, effector $CD4^+$ T cells have been further divided into two distinct lineages on the basis of their cytokine production profiles, namely Th1 and Th2. Th1 cells producing cytokines such as IL-2, IFN-γ and GM-CSF have evolved to enhance the eradication of intracellular pathogens and are thought to be potent activators of cell-mediated immunity. In contrast, Th2

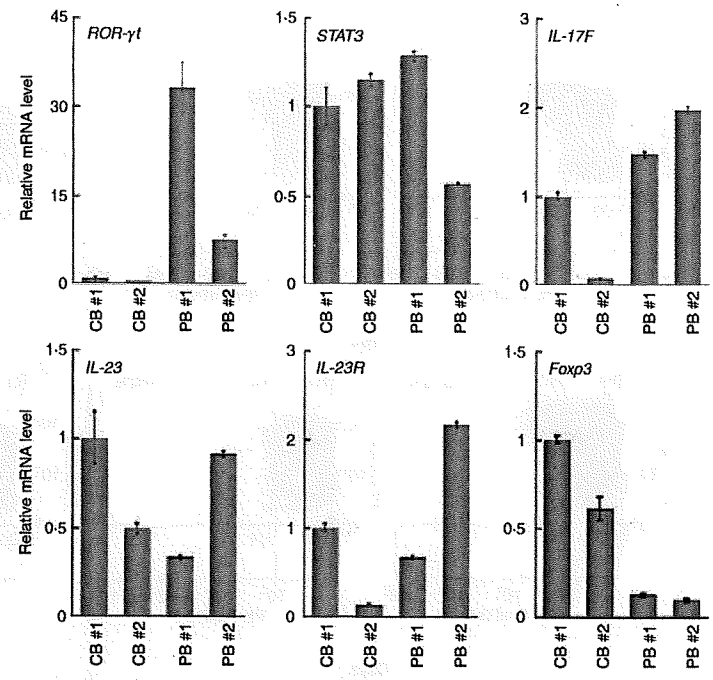

Figure 3. Quantitative polymerase chain reaction (PCR) analysis of the forkhead box protein 3 gene (*FOXP3*) and the genes related to the secretion of interleukin (IL)-17. The expression of the genes indicated was examined as in Fig 2. Data are normalized to the mRNA level in peripheral blood sample 1 (PB 1) as in Fig.2. The signal intensity was normalized using that of a control housekeeping gene [the human glyceraldehyde-3-phosphate dehydrogenase (*GAPDH*) gene]. Data are relative values with the standard deviation for triplicate wells.

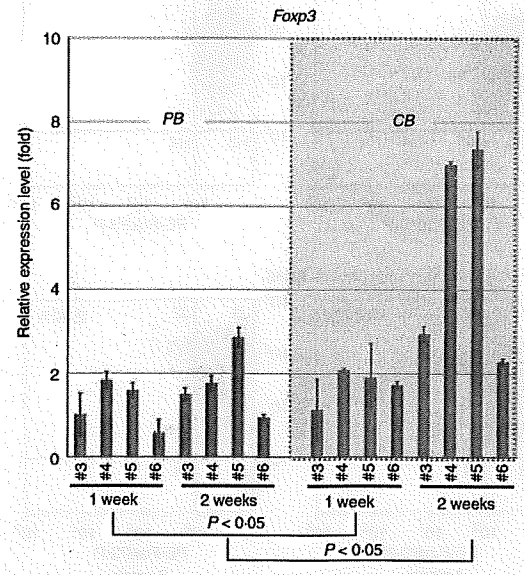

Figure 4. Quantitative polymerase chain reaction (PCR) analysis of the forkhead box protein 3 gene (*FOXP3*) in additional samples. Additional peripheral blood (PB) and cord blood (CB) samples were prepared and RNAs were extracted at 1 and 2 weeks. The expression of the *FOXP3* gene was examined as in Fig. 2. Data are normalized to the mRNA level in the sample of PB 3 at 1 week, which is arbitrarily set to 1. The signal intensity was normalized using that of a control housekeeping gene (the human β-actin gene). Data are relative values with the standard deviation for triplicate wells. The data were analysed statistically and *FOXP3* gene expression in CB-derived $CD4^+$ T cells was found to be significantly higher in comparison with equivalent PB-derived $CD4^+$ T cells at both 1 week ($P < 0{\cdot}05$) and 2 weeks ($P < 0{\cdot}05$).

cells secreting cytokines such as IL-4, IL-5, IL-6, IL-9 and IL-13 have evolved to enhance the elimination of parasitic infections and are thought to be potent activators of B-cell immunoglobulin E production, eosinophil recruitment, and mucosal expulsion. Th1-type responses to self or commensal floral antigens can promote tissue destruction and chronic inflammation, whereas dysregulated Th2-type responses can cause allergy and asthma. The development of Th1 is specified by the transcription factor T-bet (also known as Tbx-21) and master regulators of Th2 differentiation are GATA-3 and c-maf.

As shown in Fig. 2 and Table 2, the gene expression profiles of CB- and PB-derived $CD4^+$ T cells revealed no significant differences regarding cytokines related to the definition of Th1 and Th2, with the exceptions of IFN-γ and GM-CSF. The mRNA levels of IFN-γ and GM-CSF tended to be higher in CB-derived $CD4^+$ T cells than in PB-derived $CD4^+$ T cells. The mRNA expression of the transcription factors T-bet, GATA-3 and c-maf, which regulate Th1 and Th2 cell differentiation, did not differ significantly between CB- and PB-derived $CD4^+$ T cells.

In addition to Th1 and Th2 cells, IL-17 (also known as IL-17A)-producing T lymphocytes have been recently shown to comprise a distinct third subset of T helper cells, termed Th17 cells, in the mouse immune system. Th17 cells exhibit pro-inflammatory characteristics and act as major contributors to autoimmune disease. A number of experiments using animal models support a significant role for IL-17 in the response to allografts.[14,16,17] There is as yet no direct evidence for the existence of discrete Th17 cells in humans, although

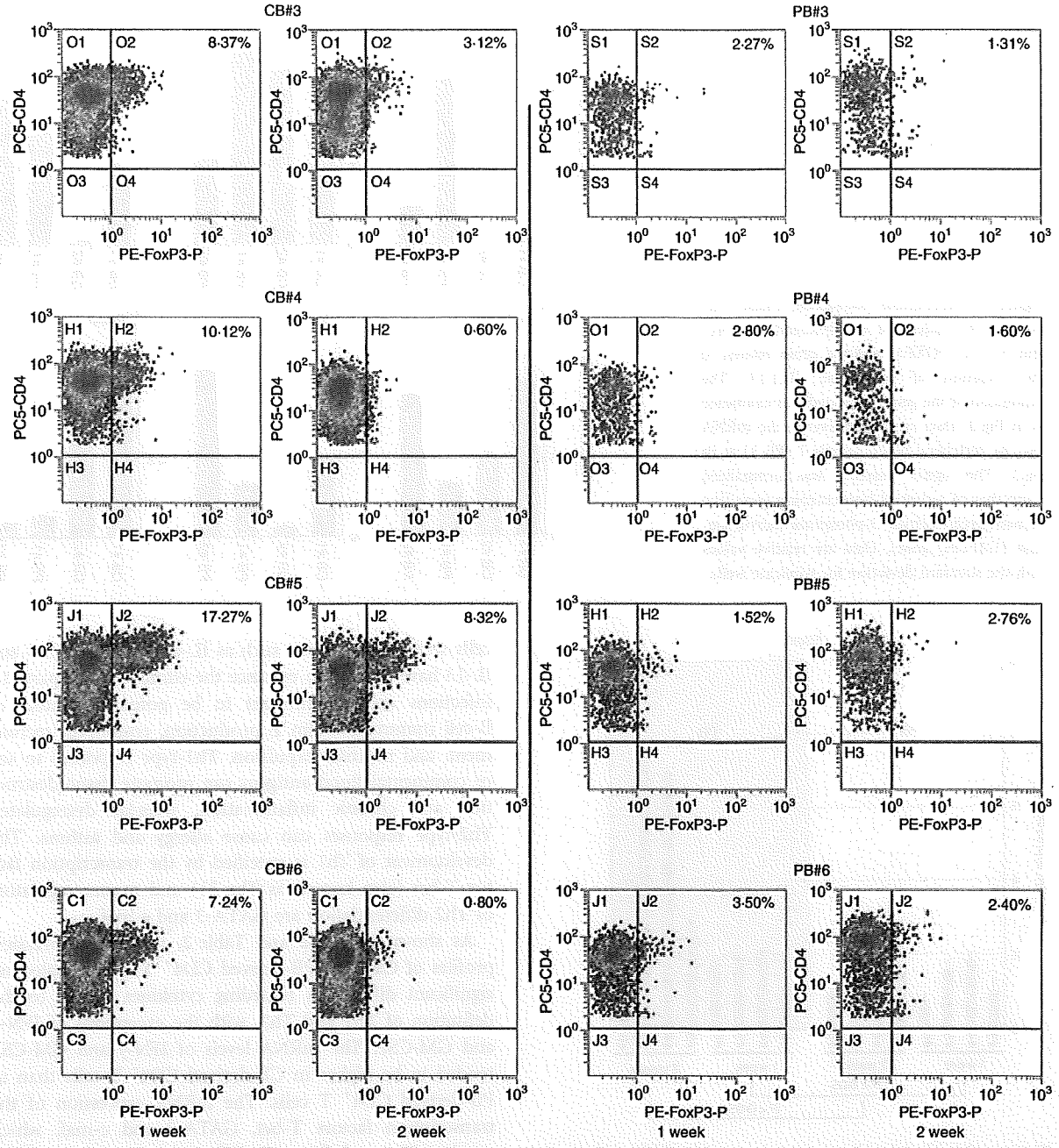

Figure 5. Protein expression of forkhead box protein 3 (Foxp3) in activated $CD4^+$ T cells. The protein expression of Foxp3 in same sample specimens as in Fig. 4 was examined by flow cytometry. The CD4 versus Foxp3 cytogram of the population gated with $CD3^+$ and $CD4^+$ in each sample is presented.

helper T cells secreting IL-17 have clearly been detected in the human immune system.[18] Several studies have shown a correlation between allograft rejection and IL-17. For example, IL-17 levels are elevated in human renal allografts during subclinical rejection and there are detectable mRNA levels in the urinary mononuclear cell sediments of these patients.[19,20] In human lung organ transplantation, IL-17 levels have also been reported to be elevated during acute rejection.[21] Interestingly, in this study, most of the PB-derived $CD4^+$ T-cell samples expressed higher levels of IL-17 mRNA than the CB-derived $CD4^+$ T-cell samples, suggesting that PB-derived $CD4^+$ T cells frequently include potent IL-17-secreting T cells.

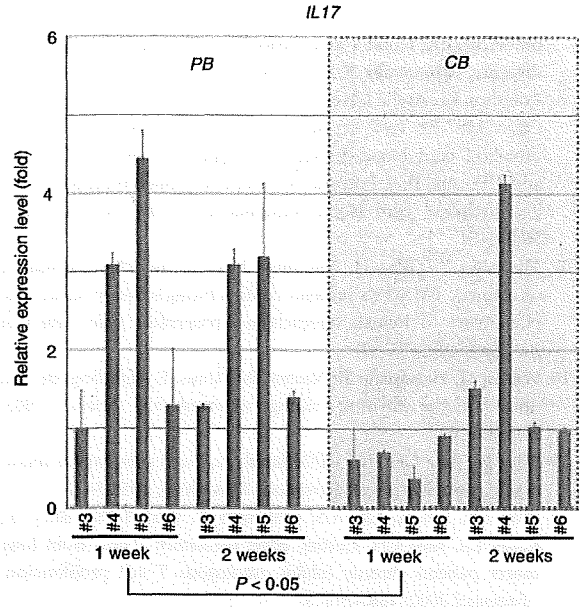

Figure 6. Quantitative polymerase chain reaction (PCR) analysis of interleukin (IL)-17 in additional samples. The expression of the *IL-17* gene in the same sample specimens as in Fig. 4 was examined and presented as in Fig 2. The data were analysed statistically and *IL-17* gene expression in peripheral blood (PB)-derived $CD4^+$ T cells was found to be significantly higher in comparison with equivalent CB-derived $CD4^+$ T cells at 1 week ($P < 0{\cdot}05$) but not at 2 weeks.

Th17 cells expand independently of T-bet or STAT-1. Ivanov *et al.*[22] have shown that the orphan nuclear receptor RORγt is the key transcription factor orchestrating the differentiation of the effector lineage. RORγt induces transcription of the gene encoding IL-17 in naïve $CD4^+$ T helper cells and is required for its expression in response to IL-6 and transforming growth factor (TGF)-β, the cytokines known to induce IL-17 expression. IL-23 is also involved in Th17 cell differentiation, but naïve T cells do not have the IL-23 receptor and are relatively refractory to IL-23 stimulation.[23,24] Although IL-23 seems to be an essential survival factor for Th17 cells, it is not required during their differentiation. It has been suggested that IL-23R expression is up-regulated on $ROR\gamma t^+$ Th17 cells in an IL-6-dependent manner. IL-23 may therefore function subsequent to IL-6/TGF-β-induced commitment to the Th17 lineage to promote cell survival and expansion and, potentially, the continued expression of IL-17 and other cytokines that characterize the Th17 phenotype. As presented in Fig. 3, the expression of the *RORγt* gene was significantly weaker in CB-derived $CD4^+$ T cells, whereas the expression of genes encoding IL-23 and the IL-23 receptor did not differ significantly between the $CD4^+$ T cells. Based on the above findings of others, it is possible that the low-level expression of the *RORγt* gene in CB-derived $CD4^+$ T cells is responsible for the absence of *IL-17* mRNA expression in those cells.

Tregs are another functional subset of T cells having anti-inflammatory properties and can cause quiescence of autoimmune diseases and prolongation of transplant function. *In vitro*, Tregs have the ability to inhibit the proliferation and production of cytokines by responder ($CD4^+$ $CD25^-$ and $CD8^+$) T cells subjected to polyclonal stimuli, as well as to down-regulate the responses of $CD8^+$ T cells, NK cells and $CD4^+$ cells to specific antigens.[25,26] These predicates translate *in vivo* to a great number of functions other than the maintenance of tolerance to self-components (prevention of autoimmune disease), such as the ability to prevent transplant rejection. Indeed, donor-specific Tregs can prevent allograft rejection in some models of murine transplant tolerance through a predominant effect on indirect alloresponses.

Foxp3 is thought to be responsible for the development of the Treg population and can act as a phenotypic marker of this fraction.[27] Tregs constitutively express CTLA-4 and there are suggestions that signalling through this pathway may be important for their function, as antibodies to CTLA-4 can inhibit Treg-mediated suppression.[28] As shown above, most of the CB-derived $CD4^+$ T cells were found to express either the *FOXP3* gene or the Foxp3 protein at higher levels compared with PB-derived $CD4^+$ T cells, suggesting that CB-derived $CD4^+$ T cells frequently include a potent Treg population.

As described above, *IL-17* mRNA was more detectable in PB-derived $CD4^+$ cells while *FOXP3* mRNA expression was higher in CB-derived $CD4^+$ cells. Post-transcriptional regulation, as well as differences in mRNA and protein turnover rates, can cause discrepancies between mRNA and protein expression and thus the differences observed in the mRNA expression do not necessary directly indicate those in protein expression.[29] Indeed, we observed some discrepancy between the levels of mRNA and protein with regard to Foxp3 expression in CB-derived $CD4^+$ T cells, as presented above. Nevertheless, changes in mRNA expression are mediated by the alteration of transcriptional regulation, and thus should indicate the differentiation ability of the cells. Therefore, our data indicate that CB-derived $CD4^+$ T cells tend frequently to include potent Tregs, while PB-derived $CD4^+$ T cells tend to include potent IL-17-secreting cells. As described above, DLI with donor CB-derived activated $CD4^+$ T cells is currently becoming established as a routine therapeutic strategy in Japan. It has been proposed that the skewing of responses towards Th17 or Th1 cells and away from Tregs may be responsible for the development and/or progression of autoimmune diseases or acute transplant rejection, and it may thus also be speculated that CB-derived $CD4^+$ T cells are more appropriate for DLI than PB-derived $CD4^+$ T cells.

However, our data also indicate the presence of individual, donor-dependent variations in the characteristics of activated $CD4^+$ T cells derived from CB and PB. More-

over, activated $CD4^+$ T cells do not consist of a single population and should include several distinct functional subsets of $CD4^+$ T cells. Therefore, it is important to clarify the characteristics of activated $CD4^+$ T cells in each preparation to predict the therapeutic effect of DLI in each clinical case.

In summary, our findings demonstrate a difference in gene expression between activated $CD4^+$ T cells derived from CB and those derived from PB. The higher level of *FOXP3* gene expression and the lower level of *IL-17* gene expression in CB-derived $CD4^+$ T cells may indicate that these cells have potential as immunomodulators in DLI therapy. Further detailed analysis should reveal the advantages of activated $CD4^+$ T cells from CB in DLI.

Acknowledgements

We thank the Tokyo Cord Blood Bank for the distribution of cord blood for research use. This work was supported by a grant from the Japan Health Sciences Foundation for Research on Publicly Essential Drugs and Medical Devices (KHC2032), Health and Labour Sciences Research Grants (the 3rd term comprehensive 10-year strategy for cancer control H19-010, Research on Children and Families H18-005, Research on Human Genome Tailor-made and Research on Publicly Essential Drugs and Medical Devices H18-005), and a Grant for Child Health and Development from the Ministry of Health, Labour and Welfare of Japan. It was also supported by CREST, JST.

Disclosures

No competing personal or financial interests exist for any of the authors in relation to this manuscript.

References

1 Loren AW, Porter DL. Donor leukocyte infusions after unrelated donor hematopoietic stem cell transplantation. *Curr Opin Oncol* 2006; **18**:107–14.
2 Roush KS, Hillyer CD. Donor lymphocyte infusion therapy. *Transfus Med Rev* 2002; **16**:161–76.
3 Alyea EP, Soiffer RJ, Canning C *et al.* Toxicity and efficacy of defined doses of CD4(+) donor lymphocytes for treatment of relapse after allogeneic bone marrow transplant. *Blood* 1998; **91**:3671–80.
4 Giralt S, Hester J, Huh Y *et al.* CD8-depleted donor lymphocyte infusion as treatment for relapsed chronic myelogenous leukemia after allogeneic bone marrow transplantation. *Blood* 1995; **86**:4337–43.
5 Tomizawa D, Aoki Y, Nagasawa M *et al.* Novel adopted immunotherapy for mixed chimerism after unrelated cord blood transplantation in Omenn syndrome. *Eur J Haematol* 2005; **75**:441–4.
6 Cohena Y, Nagler A. Hematopoietic stem-cell transplantation using umbilical-cord blood. *Leuk Lymphoma* 2003; **44**:1287–99.
7 Parmar S, Robinson SN, Komanduri K *et al.* Ex vivo expanded umbilical cord blood T cells maintain naive phenotype and TCR diversity. *Cytotherapy* 2006; **8**:149–57.
8 Robinson KL, Ayello J, Hughes R, van de Ven C, Issitt L, Kurtzberg J, Cairo MS. Ex vivo expansion, maturation, and activation of umbilical cord blood-derived T lymphocytes with IL-2, IL-12, anti-CD3, and IL-7. Potential for adoptive cellular immunotherapy post-umbilical cord blood transplantation. *Exp Hematol* 2002; **30**:245–51.
9 Miyagawa Y, Okita H, Nakaijima H *et al.* Inducible expression of chimeric EWS/ETS proteins confers Ewing's family tumor-like phenotypes to human mesenchymal progenitor cells. *Mol Cell Biol* 2008; **28**:2125–37.
10 Werlen G, Hausmann B, Naeher D, Palmer E. Signaling life and death in the thymus: timing is everything. *Science* 2003; **299**:1859–63.
11 Riley JL, June CH. The CD28 family: a T-cell rheostat for therapeutic control of T-cell activation. *Blood* 2005; **105**:13–21.
12 Woo EY, Yeh H, Chu CS, Schlienger K, Carroll RG, Riley JL, Kaiser LR, June CH. Cutting edge: regulatory T cells from lung cancer patients directly inhibit autologous T cell proliferation. *J Immunol* 2002; **168**:4272–6.
13 Azuma H, Yamada Y, Shibuya-Fujiwara N *et al.* Functional evaluation of ex vivo expanded cord blood lymphocytes: possible use for adoptive cellular immunotherapy. *Exp Hematol* 2002; **30**:346–51.
14 Afzali B, Lombardi G, Lechler RI, Lord GM. The role of T helper 17 (Th17) and regulatory T cells (Treg) in human organ transplantation and autoimmune disease. *Clin Exp Immunol* 2007; **148**:32–46.
15 Castellino F, Germain RN. Cooperation between CD4+ and CD8+ T cells: when, where, and how. *Annu Rev Immunol* 2006; **24**:519–40.
16 Reiner SL. Development in motion: helper T cells at work. *Cell* 2007; **129**:33–6.
17 Bi Y, Liu G, Yang R. Th17 cell induction and immune regulatory effects. *J Cell Physiol* 2007; **211**:273–8.
18 Fossiez F, Djossou O, Chomarat P *et al.* T cell interleukin-17 induces stromal cells to produce proinflammatory and hematopoietic cytokines. *J Exp Med* 1996; **183**:2593–603.
19 Loong CC, Hsieh HG, Lui WY, Chen A, Lin CY. Evidence for the early involvement of interleukin 17 in human and experimental renal allograft rejection. *J Pathol* 2002; **197**:322–32.
20 Van Kooten C, Boonstra JG, Paape ME *et al.* Interleukin-17 activates human renal epithelial cells in vitro and is expressed during renal allograft rejection. *J Am Soc Nephrol* 1998; **9**:1526–34.
21 Vanaudenaerde BM, Dupont LJ, Wuyts WA *et al.* The role of interleukin-17 during acute rejection after lung transplantation. *Eur Respir J* 2006; **27**:779–87.
22 Ivanov II, McKenzie BS, Zhou L, Tadokoro CE, Lepelley A, Lafaille JJ, Cua DJ, Littman DR. The orphan nuclear receptor RORgammat directs the differentiation program of proinflammatory IL-17+ T helper cells. *Cell* 2006; **126**:1121–33.
23 Langrish CL, Chen Y, Blumenschein WM *et al.* IL-23 drives a pathogenic T cell population that induces autoimmune inflammation. *J Exp Med* 2005; **201**:233–40.
24 Oppmann B, Lesley R, Blom B *et al.* Novel p19 protein engages IL-12p40 to form a cytokine, IL-23, with biological activities similar as well as distinct from IL-12. *Immunity* 2000; **13**: 715–25.

25 Dieckmann D, Plottner H, Berchtold S, Berger T, Schuler G. Ex vivo isolation and characterization of CD4(+) CD25(+) T cells with regulatory properties from human blood. *J Exp Med* 2001; **193**:1303–10.

26 Wing K, Lindgren S, Kollberg G, Lundgren A, Harris RA, Rudin A, Lundin S, Suri-Payer E. CD4 T cell activation by myelin oligodendrocyte glycoprotein is suppressed by adult but not cord blood CD25+ T cells. *Eur J Immunol* 2003; **33**:579–87.

27 Wan YY, Flavell RA. Identifying Foxp3-expressing suppressor T cells with a bicistronic reporter. *Pro Natl Acad Sci USA* 2005; **102**:5126–31.

28 Read S, Greenwald R, Izcue A, Robinson N, Mandelbrot D, Francisco L, Sharpe AH, Powrie F. Blockade of CTLA-4 on CD4+ CD25+ regulatory T cells abrogates their function in vivo. *J Immunol* 2006; **177**:4376–83.

29 Hack CJ. Integrated transcriptome and proteome data: the challenges ahead. *Brief Funct Genomic Proteomic* 2004; **3**:212–9.

Int J Hematol
DOI 10.1007/s12185-009-0408-0

ORIGINAL ARTICLE

Phenotypic variations between affected siblings with ataxia-telangiectasia: ataxia-telangiectasia in Japan

Tomohiro Morio · Naomi Takahashi · Fumiaki Watanabe · Fumiko Honda · Masaki Sato · Masatoshi Takagi · Ken-ichi Imadome · Toshio Miyawaki · Domenico Delia · Kotoka Nakamura · Richard A. Gatti · Shuki Mizutani

Received: 26 May 2009 / Revised: 31 July 2009 / Accepted: 3 August 2009

Abstract A nationwide survey was conducted for identifying ataxia-telangiectasia (AT) patients in Japan. Eighty-nine patients were diagnosed between 1971 and 2006. Detailed clinical and laboratory data of 64 patients including affected siblings were collected. Analyses focused on malignancy, therapy-related toxicity, infection, and hematological/immunological parameters. The phenotypic variability of AT was assessed by comparing 26 affected siblings from 13 families. Malignancy developed in 22% of the cases and was associated with a high rate of severe therapy-related complications: chemotherapy-related cardiac toxicity in 2 children, and severe hemorrhagic cystitis requiring surgery in 2 patients. The frequency of serious viral infections correlated with the T cell count. Hypogammaglobulinemia with hyper-IgM (HIGM) was recorded in 5 patients, and 3 patients developed pan-hypogammaglobulinemia. Differences in immunological parameters were noted in siblings. Four patients showed an HIGM phenotype, in contrast to their siblings with normal IgG and IgM levels. The patients with HIGM phenotype showed reduced levels of TRECs and $CD27^{+}CD20^{+}$ memory B cells. The findings suggest that hitherto unidentified modifier genes or exogenous environmental factors can influence the overall immune responses. Our data along with future prospective study will lead to better understanding of the hematological/immunological phenotypes and to better care of the patients.

Keywords Ataxia-telangiectasia · Phenotypic variations · Hyper-IgM · Modifier genes · Affected siblings

T. Morio (✉) · N. Takahashi · F. Watanabe · F. Honda · M. Sato · M. Takagi · S. Mizutani
Department of Pediatrics and Developmental Biology, Tokyo Medical and Dental University Graduate School of Medical and Dental Sciences, 1-5-45 Yushima, Bunkyo-ku, Tokyo 113-8519, Japan
e-mail: tmorio.ped@tmd.ac.jp

K. Imadome
Department of Infectious Diseases, National Research Institute for Child Health and Development, Tokyo, Japan

T. Miyawaki
Department of Pediatrics, Toyama University School of Medicine, Toyama, Japan

D. Delia
Department of Experimental Oncology, Istituto Nazionale Tumori, Milan, Italy

K. Nakamura · R. A. Gatti
Department of Pathology and Laboratory Medicine, David Geffen School of Medicine, University of California, Los Angeles, CA, USA

1 Introduction

This is the first survey with regard to ataxia-telangiectasia (AT) carried out in Japan.

AT is a rare genetic disorder having multiple manifestations. It is characterized by early-onset of progressive neurodegeneration, oculocutaneous telangiectasia, various immunodeficiencies leading to a predisposition to infection, high risk of developing lymphoreticular malignancy, and increased sensitivity to ionizing radiation. Characteristic laboratory and diagnostic findings include cerebellar atrophy, high serum alpha-fetoprotein (AFP) level, and chromosomal translocations involving immunoglobulin and T cell receptor genes [1–5].

Clinical heterogeneity is observed within the disorder [1, 3, 5–8]. Neurological symptoms include cerebellar ataxia, oculomotor apraxia, disarthria, and choreoathetosis,

Published online: 25 August 2009

which range from classical form with steady progression to milder forms with milder phenotype or slower progression.

Predisposition to infection because of impaired immunity is noted; however, it is variable [1, 4, 6]. Lower respiratory infections increase with age, partly as a consequence of food aspiration caused by deterioration of neurological functions.

The immune defect is rarely progressive and is variable among AT patients [1, 8, 9]. The common humoral abnormalities are decreased levels of IgA, IgE, and IgG2. The most notable defect in T cell immunity is lymphopenia, especially in the CD4 T cell population; however, 30% of patients do not show immunodeficiency [8].

Following cloning of a gene responsible for AT, diagnosis of AT could be confirmed by measuring ATM protein, ATM kinase activity, or by sequencing the ataxia-telangiectasia mutated (*ATM*) gene [2, 10, 11]. ATM plays a controlling role in (1) recognition and repair of DNA damage by interaction with H2AX, Mre11/Rad50/NBS1, and SCM1; (2) cell cycle arrest by phosphorylation of various molecules, including Brca1, Chk2, and E2F1; and (3) cellular apoptosis via MDM2 and the p53 pathway [3, 12–14].

Despite progress in identification of the molecular basis of ATM function, little research evidence is available concerning the pathogenesis of AT or therapies that might aid the AT patients [15–18]. This reflects the relative rarity of this disorder, and thus the paucity of data from large patient cohorts. Particularly, the severe adverse effects of chemotherapeutic agents leading to increased DNA damage in AT patients with malignancies need further scrutiny.

This prompted us to conduct a nationwide survey in Japan with regard to AT, and to collect data on the clinical signs/symptoms, long-term follow-up laboratory data, and complications of treatment. Basic immunological studies were performed on patients currently alive. We reassessed the disease survival rate and compared the data from affected siblings to determine the phenotypic variability between patients with similar genotypes and environments. We describe here therapy-related toxicity, hematological/immunological changes, and phenotypic diversity in the affected siblings.

2 Methods

2.1 Patients and questionnaire

In September 2005, a preliminary questionnaire soliciting information about AT patients was sent to 1,223 departments of 665 medical hospitals/institutes in Japan. A more extensive questionnaire was conducted for 92 potential AT patients. Eighty-nine patients were enrolled in this analysis after elimination of non-AT patients and overlapping information; and detailed information was obtained from the remaining 64 patients. The data were provided after obtaining informed consent from the patients currently alive or their parents.

AT diagnosis of patients was conducted at their respective institutes and reconfirmed at our institute by assessing the clinical symptoms, laboratory findings, and carrying out genetic analysis, protein expression analysis, or both in some cases. The study included 28 sibling cases, of which 26 patients from 13 families were subjected to comparative analysis.

2.2 Western blotting

In order to prepare cellular extracts for anti-ATM immunoblotting, the T cells from the AT patients were expanded in the presence of recombinant IL-2 (700 IU/mL; Proleukin, Chiron, Amsterdam, Netherland) in a flask with immobilized anti-CD3 mAb:OKT3 (5 μg/mL, Janssen-Kyowa, Tokyo, Japan). Western blotting with anti-ATM antibody was performed as previously described [19, 20].

Mutational analysis was performed as described previously [21, 22] and will be reported in a separate paper. The analyses were approved by the ethics committee of our university, and written informed consent was obtained from the patients and/or their parents.

2.3 Immunological characterization

Surface immunophenotyping was performed as previously described [23–25]. Data for T cell-receptor excision circles (TRECs) were calculated using peripheral mononuclear cells as described previously [26]. The quality of the extracted DNA was confirmed by the measurement of GAPDH, and TRECs level was expressed as copy number/μgDNA.

2.4 Statistical analysis

The probability of survival was estimated by the product-limit method. Student's *t* test was applied for statistical analysis between the two groups.

3 Results

3.1 Diagnosis and survival

The median age at diagnosis was 6.7 years (range 0.9–24.5 years), and the median age of survival was 26.0 years (Fig. 1). Twenty-nine patients had died before the study began, at a median age of 19.7 years (range 5.8–31.8 years).

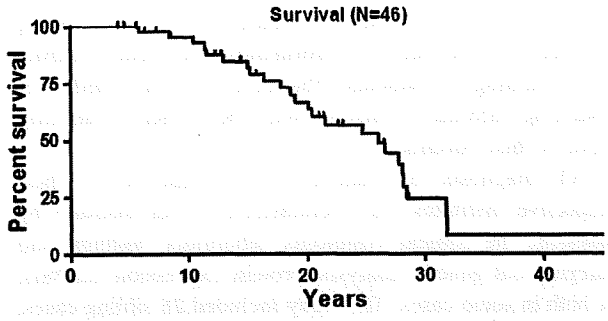

Fig. 1 Survival rates of 46 ataxia-telangiectasia (AT) patients. Survival rates of 46 patients as calculated by Kaplan–Meier method. The median survival was 26 years

The most frequently documented cause of death was infection (18 patients), and 5 of 18 patients died of infection during chemotherapy for malignancy. In the remaining 11 patients, 3 patients died of malignancy, 5 patients from various other causes, and 3 from unknown etiology.

The median age of the patients currently alive was 15.0 years (range 4–28.6 years). The median age of onset of telangiectasia was recorded as 6.7 years (range 1.8–13.5 years). Clinical characteristics of the patients are displayed in Table 1.

3.2 Neurological symptoms

Neurological symptoms are summarized in Table 1. Tremor, oculomotor apraxia, and chorea were observed in 68, 59, and 27% of the patients, respectively. Thirty of 45 patients were wheelchair-bound at the median age of 8.0 years (range 2.5–16.4 years).

3.3 Malignancies

Detailed information was obtained from 12 patients with malignancy. Of these patients, 6 had acute lymphoblastic leukemia (ALL; 4 T-ALL and 2 Precursor-B-ALL), 4 had non-Hodgkin lymphoma, 1 had Langerhans cell histiocytosis, and 1 developed cholangiocarcinoma. Two patients achieved long-term complete remission, 3 died of tumor progression, 4 died of bacterial infections during chemotherapy, and 1 died of cytomegalovirus (CMV) infection during the period of chemotherapy-related immunodeficiency. One patient died as a result of infection before starting therapy, and 1 patient died because of cardiac failure due to chemotherapy.

Altogether two patients with T-ALL suffered from the left cardiac failure caused by chemotherapy that included anthracycline. During maintenance therapy with methotrexate and 6-mercaptoprine, 1 patient with precursor-B-ALL developed inflammation of multiple lymph nodes with NK-cell cytosis which rapidly developed into multiple organ failure. Although the definitive diagnosis was not made, this was probably due to EBV-associated NK-cell lineage proliferative disorder.

Hemorrhagic cystitis requiring surgical intervention was noted in 2 patients. One patient with idiopathic thrombocytopenic purpura (ITP) refractory to gammaglobulin treatment and steroid therapy, received intravenous cyclophosphamide. Although the patient maintained a platelet level >50,000/mm^3, massive hemorrhage in the bladder developed 3 years after completing cyclophosphamide therapy. This patient also suffered from acute nephritis accompanied by acute renal failure before developing ITP [27]. The second patient received a cyclophosphamide-containing regimen for the treatment of ALL, and

Table 1 Patient characteristics

Male/female	40/40
Sibling cases/patients without a sibling	28/52
Maternal breast cancer	2.2% (1/46)
Age at diagnosis (age, years): median (range)	6.7 (0.9–24.5)
Alive/deceased	28/29
Median age of survival: median (range)	26.0 (5.8–31.8)
Onset of telangiectasia (age, years): median (range)	6.7 (1.8–13.5)
Neurological symptoms	
Onset of ataxia (age, years): median (range)	1.5 (0.5–5.6)
Ataxia	100% (80/80)
Apraxia	59% (26/44)
Chorea	27% (12/44)
Infections (number)	
Bacterial infection	29
Severe viral infection	11
Malignancy	22% (17/76)
Acute leukemia	6
Lymphoma	4
Langerhans cell histiocytosis	1
Cholangiocarcinoma	1
Unknown	5
Glucose intolerance	17% (8/46)
Growth retardation (height <2.0 SD at >6 years)	86% (19/22)
Hypothyroidism	0%
Other clinical symptoms	
Hemorrhagic cystitis (post-chemotherapy)	2
Cardiac failure (post-chemotherapy)	2
Acute nephritis/renal failure	1
Heart failure	1
Paroxysmal supraventricular tachycardia	1
ITP	1

Eighty-nine patients were enrolled in this analysis; and detailed information was obtained in 64 patients. Positive in the total numbers of the reply is indicated in parenthesis when % is calculated. Total number in each reply does not add up to 89 or to 64, since not all the question items were answered

developed massive hemorrhage during maintenance therapy with methotrexate and 6-mercaptopurine. Cytoscopy revealed varicose veins in the bladder of both of the patients.

3.4 Infections

Twenty-nine patients had bacterial infections mainly of the sinus or the lower respiratory tract. Eleven patients had severe or persistent viral infections, of which 3 suffered from chronic Epstein-Barr virus (EBV) infection, 2 from severe recurrent varicella-zoster virus (VZV) infection, 2 from severe measles pneumonia, 1 from herpes simplex virus (HSV) encephalitis, and 1 from systemic CMV infection after a treatment course for T-ALL. $CD3^+$T cell counts were known in 7 patients and were less than 450/mm^3 in 5 patients. T cell-lymphopenia did not result from chemotherapy for malignancy. One of the patients had EBV infection after completion of therapy for malignant lymphoma.

Anti-EBV titers were documented in 19 patients. Five had anti-EBV titers indicative of persistently active EBV infection: elevated VCA IgG (>1,280×) and EA-DR IgG (>40×). Of the 5 patients, 4 showed negative anti-EBNA antibody (<10×) and 1 had a normal EBNA response (40×).

None of the patients in this cohort had fungal infections caused by agents such as *Candida, Aspergillus,* or *Pneumocystis jerovicii,* or protozoal infections.

3.5 Hematological and immunological data

Serum AFP level was elevated in 43 of the 44 patients tested. The median serum concentration of AFP was 372 ng/mL (range 71–1,518).

Average neutrophil count, lymphocyte count, hemoglobin levels, and platelet levels were 5,620/mm^3, 1,610/mm^3, 13.0 g/dL, and 40.2 × 10^4/mm^3, respectively. Data on lymphocyte subsets were recorded in 29 patients. $CD3^+$T cell count was <1,000/mm^3 in 24 patients and was decreased (>2 SD below the mean for age) in 66% of patients. $CD4^+$T cells, $CD8^+$T cells, and $CD20^+$B cells were decreased in 76, 39, and 78% of patients, respectively. Distribution of each subset is shown in Fig. 2. The TRECs were measured in mononuclear cells of 12 patients, and were significantly lower than those in age-matched controls (Fig. 3) in concordance with previously reported data [9, 28]. There was no correlation between the $CD3^+$T cell counts and the TRECs levels (data not shown).

Five of ten patients with ≤450/mm^3 $CD3^+$lymphocytes, whereas 2 out of 19 patients with >450/mm^3 $CD3^+$T cells developed severe viral infection ($p < 0.05$).

Immunoglobulin levels were evaluated in 50 patients (Fig. 4). Four patients (8%) showed elevated IgM level

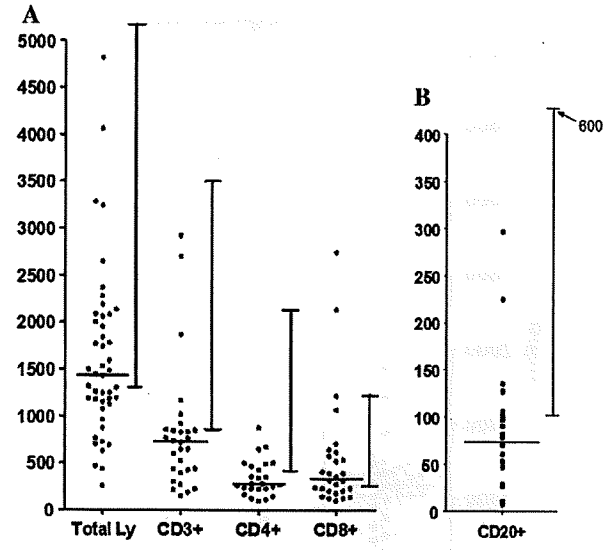

Fig. 2 Lymphocyte counts of patients with AT. Total lymphocytes, $CD3^+$, $CD4^+$, $CD8^+$ (**a**) and $CD20^+$ cell counts (**b**) are shown. *Horizontal bar* shows median value of the cell counts. Normal ranges (5th–95th percentiles) for patients aged 10 years to adults are shown on the *right side* of each column

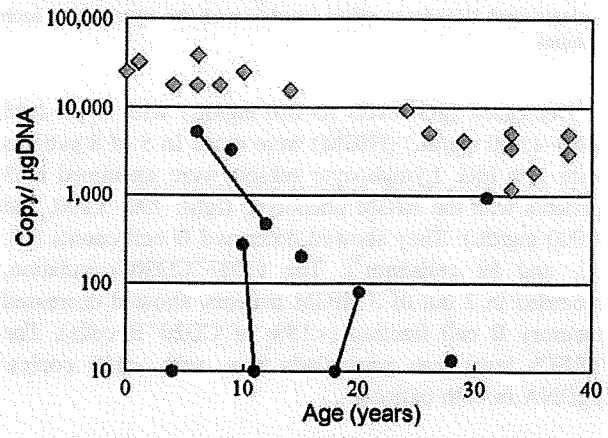

Fig. 3 Quantification of T cell receptor excision circles (TRECs) in AT patients. *Closed diamonds* show TRECs in normal healthy subjects. *Closed circles* are TRECs measured in AT patients. *Solid lines* connect data for affected siblings

(>450 mg/dL) with normal or elevated IgG level (1,050–2,513 mg/dL). Three patients showed normal IgA level, and 1 patient showed absence of IgA. Whether they had polyclonal or monoclonal gammopathy is not known. IgG level was <500 mg/dL in 8 patients. Reduced serum levels of IgG and IgM were recorded in 3 patients on more than 2 separate occasions. Two of the 3 patients developed hematological malignancy thereafter. Serum IgA level was below 50 mg/dL in 17 patients (34%), of which 10 patients had isolated IgA deficiency.

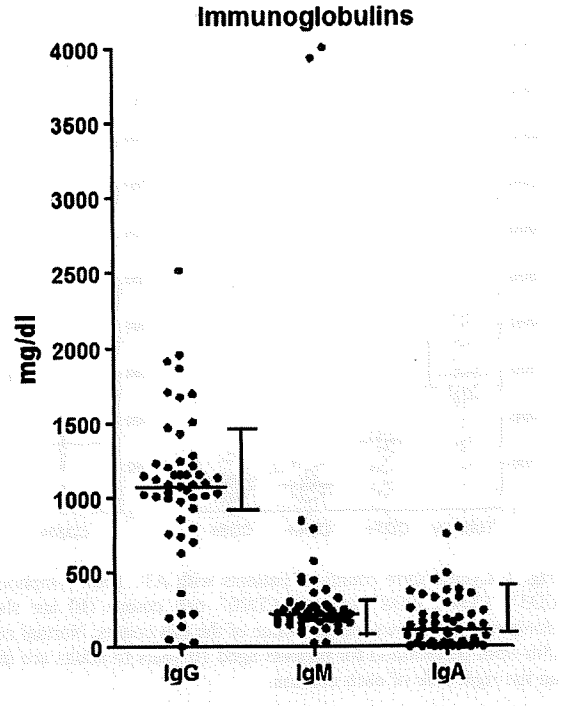

Fig. 4 Serum IgG, IgM, and IgA levels of AT patients. *Horizontal bar* shows median value. Normal ranges (5th–95th percentiles) for patients aged 10 years to adults are shown on the *right side* of each column

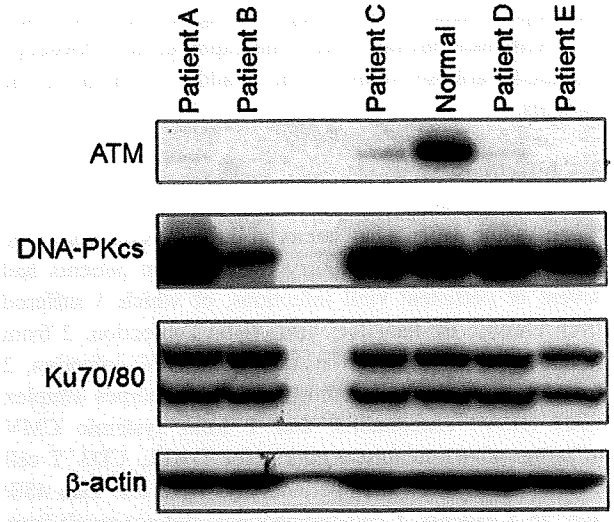

Fig. 5 Western blot analysis for ATM. Protein extracted from activated T cells from normal subjects and from clinically diagnosed AT patients (*Patient A*, *B*, *C*, *D*, and *E*) were subjected to Western blot analysis for ATM. The blots were also probed with antibodies to DNA-PKcs, Ku70/80, and to *β*-actin

Decreased IgG levels (0–220 mg/dL) with hyper-IgM (380–4,000 mg/dL) (HIGM) were noted in 5 of 8 patients with low IgG. Lymphocyte subsets were examined in 3 patients with the HIGM phenotype (IgM: 790, 3,800, and 4,000 mg/dL). They showed decreased B cell counts (10, 52, and 82 cells/mm^3). The CD27$^+$CD20$^+$population, recorded in 2 out of 3 HIGM patients, showed decreased memory B cell fraction (<15% of CD20$^+$B cells). The TRECs level was particularly low, with <100 copies/μgDNA in both patients.

3.6 Comparison of phenotypes in affected siblings

Phenotypic description and laboratory data from 13 pairs of affected siblings were collected at comparable age whenever possible. Sequencing and Western blot analyses were performed in 6 families. ATM mutations were different in all families (manuscript in preparation), and ATM expression was virtually absent (<2% of normal ATM level) in all the cases. The results of anti-ATM Western blot for representative patients are shown in Fig. 5.

Some neurological and endocrinological findings were concordant in AT siblings. Chorea was noted in 5 patients. Two sibling pairs were concordant. In another family, only a younger brother showed chorea. Diabetes mellitus was detected in 5 siblings in 3 families.

Differences were noted in some associated symptoms and laboratory data (Table 2). Serum AFP level was more than three times higher in the elder sibling in 2 sibling pairs, higher in the younger sibling in 2 families, and almost at the same level in 6 sibling pairs. In 2 siblings, the elder brother had acute nephritis, ITP, hemorrhagic cystitis, and was obese, with an elevated serum triglyceride level (>400 mg/dL), whereas a younger brother was emaciated with a low triglyceride level (<30 mg/dL) with none of the disorders of his brother.

A large variation was noted in hematological and immunological parameters (Table 2). In 3 families, the lymphocyte count was consistently more than three times higher in one sibling than the other sibling (>2,000/mm^3). Decreased IgG/IgA with hyper-IgM was recorded in 4 patients. HIGM was detected before the age of 2 years in 3 patients, and was recorded at the age of 10 years in 1 patient, whereas it was not observed in their siblings: IgG/IgM/IgA levels were normal in 3 patients, and 1 patient showed only decreased IgA. Except for 3 patients with HIGM, 3 patients had low serum IgA levels, while the IgA levels of their siblings were normal or elevated.

No significant differences were observed in the CD3$^+$, CD4$^+$, CD8$^+$, or CD20$^+$ counts in the sibling pairs. TRECs were measured in 6 siblings from 3 families. Slight differences were observed in TRECs values; however, this could be because of the age difference.

Common features of AT patients with HIGM phenotype were low memory B cell count and low TRECs level. The CD27$^+$CD20$^+$memory B cell/CD27$^-$CD20$^-$naïve B cell ratio was 0.2/1.5% in 1 patient with HIGM, while that of

Table 2 Multiparameter analysis of affected siblings

Patient	Age (years)	Ly (mm^3)	Plt ($\times 10^3/mm^3$)	AFP (ng/mL)	T-chol (mg/dL)	TG (mg/dL)	IgG (mg/dL)	IgM (mg/dL)	IgA (mg/dL)	IgE (ng/mL)	Died (age)
Normal range		1,300–5,300	100–400	<10	150–220	50–150	800–1,600	50–280	100–400	0–380	
1 EB	8.3	3,280	323	n.t.	n.t.	n.t.	**220**	**436**	**0**	n.t.	10.5
1 YB	8.0	1,740	395	135	147	n.t.	**1,000**	**150**	**238**	68	15.0
2 ES	20.0	2,130	380	525	187	n.t.	1,464	360	140	280	20.0
2 YS	9.6	3,240	n.t.	690	160	n.t.	1,008	215	328	68	20[b]
3 EB	11.9	**4,060**	334	**1,090**	177	n.t.	1,130	224	0.8	0	20.4
3 YB	7.5	**1,185**	n.t.	**273**	n.t.	n.t.	1,240	274	0.8	0	14[b]
4 ES	13.7	1,950	329	529	223	n.t.	1,502	239	**30**	n.t.	15.0
4 YS[a]	19.2	1,590	417	524	164	100	1,860	278	**749**	<1	28.2
5 TwB	27.3	1,530	426	n.t.	186	n.t.	n.t.	n.t.	n.t.	n.t.	28.6 (A)
5 TwB	27.3	2,060	492	n.t.	n.t.	n.t.	n.t.	n.t.	n.t.	n.t.	28.6 (A)
6 EB	16.8	1,260	423	316	n.t.	n.t.	1,950	266	**163**	7 IU/mL	22.6 (A)
6 YB	10.8	1,130	504	n.t.	n.t.	n.t.	1,690	256	**2**	<4 IU/mL	16.6[b]
7 ES[a]	11.7	1,250	620	**949**	167	195	852	257	**369**	<1	12.8 (A)
7 YB[a]	5.2	1,180	422	**226**	209	67	1,095	300	**24**	<1	6.3 (A)
8 ES	24.0	1,780	465	**420**	n.t.	n.t.	700	250	179	n.t.	19.0
8 YB	19.0	1,300	n.t.	**1,518**	n.t.	n.t.	755	122	213	<2.0	26.5 (A)
9 EB[a]	19.6	1,320	324	838	177	100	1,144	104	111	14	21.0 (A)
9 YB[a]	17.2	1,500	533	632	144	150	793	89	329	0.9	18.6 (A)
10 ES	11.8	700	429	560	186	66	1,120	224	128	n.t.	28.1
10 YS	9.8	690	490	560	209	121	1,150	168	80	n.t.	31.7
11 ES	4.0	**2,280**	212	100	143	95	**1,703**	**190**	64	<30	5.8
11 YS[a]	3.4	**460**	149	93	125	104	**136**	**3,932**	75	<1	4.0 (A)
12 EB[a]	10.6	**4,820**	**75**	296	117	**499**	**50**	**4,000**	**10**	1	11.6 (A)
12 YB[a]	8.9	**1,070**	**251**	357	133	**22**	**1,070**	**191**	**346**	3	9.7 (A)
13 ES	24.4	730	**454**	**292**	175	88	**<5**	**790**	**<5**	**<5**	24.7
13 YS[a]	22.9	1,250	**374**	**1,662**	197	97	**991**	**263**	**191**	n.t.	23.0 (A)

Ly lymphocytes, *TG* triglyceride, *EB* elder brother, *ES* elder sister, *YB* younger brother, *YS* younger sister, *TwB* twin brother, *n.t.* not tested, *A* alive

[a] Mutation in ATM gene was confirmed

[b] The age of the patient at his/her last visit. Bold indicates data where difference among siblings was noted

his brother was 2.1/4.4%. Decrease in the memory B cell fraction was noted in another patient with HIGM (0.9/10.9%). Unfortunately, lymphocyte immunophenotyping of the patient's elder sister could not be recorded because of her early death from leukemia.

4 Discussion

Toxicity of antineoplastic agents was highlighted as an important issue for treating malignancy in AT patients. Two patients in our cohort developed left cardiac failure after an anthracycline-containing therapeutic regimen. Hemorrhagic cystitis was observed in 2 patients. Anecdotal reports suggest that telangiectasia can occur in the bladder wall; however, symptoms resulting from telangiectasia have only been recently reported in one case who had a history of nephritis and ITP [27, 29]. Our data show that this was not because of peculiarity of the reported patient. The cystitis was most likely related to late toxicity of cyclophosphamide. Although hemorrhagic cystitis is the common adverse effect of high-dose cyclophosphamide, it occurs in less than 5% of patients receiving the conventional dose. Severe cyclophosphamide-related cystitis that requires surgical intervention is rare. Hematuria might begin immediately or occur several years following treatment [30–32]. Therefore, the physicians should be aware of the late side effects of cyclophosphamide administered to AT patients.

Half of the AT patients developing malignancy died of infection or therapy-related toxicity, while 7 of 10 AT patients developed lymphoid malignancy after the age of

9 years, 2 developed B cell malignancy before the age of 6 years (at 4 and 5.7), when diagnosis of AT was not yet established. Both patients died of therapy-related toxicity. To improve early diagnosis of AT, routine measurement of AFP is strongly recommended on diagnosis of B cell malignancy in ataxic children. This would help in finding AT patients who have developed ALL and would require dose modification upon the treatment. Supervision by an oncologist familiar with the specific problems encountered by AT patients would also be beneficial for treatment of malignancy in AT patients.

Severe viral infection has not been a hallmark of AT children in previous surveys, despite their defective antibody response and impaired cellular immunity [8]. Of the 11 patients with severe viral infections, 7 had infections caused by herpesvirus species (3 EBV, 2 VZV, 1 CMV, and 1 HSV). Reduced $CD3^{+}$T cell counts with the absence of lymphopenia or hypogammaglobulinemia were noted in 5 patients, suggesting that those with T-lymphopenia are susceptible to herpesvirus infection.

It is of interest that 5 AT patients showed abnormal anti-EBV titers indicative of persistently active EBV infection, among whom 3 patients also displayed clinical symptoms of EBV infection. Further prospective large-scale study is warranted to investigate immunity against the herpesvirus species in AT children [33].

HIGM phenotype indicative of defective class switch recombination (CSR) has been documented in AT patients; however, it is considered to be infrequent, and its incidence was hitherto unknown. ATM protein is involved in CSR [34–38]. The CSR junctions in B cells from AT patients show a dependence on microhomologies and are devoid of normally occurring mutations around the breakpoint. In our study, AT patients showed deficiencies of serum IgA (in 60% of the patients), IgE (in 80%), IgG (in 26%), and IgG2 (in 80%).

In a previous study, 8% of AT patients developed dysgammaglobulinemia with gammopathy. In our study, 8 patients (16%) showed decreased serum IgG and IgA/E levels. Panhypogammaglobulinemia was documented in 3 patients. It should be noted that 2 of 3 patients with panhypogammaglobulinemia developed lymphoid malignancy. Five patients in our study (10%) showed the HIGM phenotype, and 3 of them showed markedly elevated serum IgM with low IgG level (<200 mg/dL). In fact, 1 patient was initially diagnosed with female HIGM syndrome with mild ataxia. Recent study has shown the immunological phenotype could be reminiscent of hyper-IgM syndrome in patients with AT [27, 39], and our study has shown the hyper-IgM phenotype is not rare in the patients.

Further immunological data were available for 4 of 5 AT patients with HIGM. Some aspects of their data are informative for considering possible mechanisms of the CSR defect. First, HIGM was observed at early childhood before development of bacterial/viral infection. Second, 4 AT patients with HIGM had siblings with AT, and they showed normal IgG/M levels. Third, TRECs in 2 HIGM-AT patients were especially low with <100 TRECs/μgDNA. These data indicate that the HIGM phenotype was not determined solely by ATM mutation type or by the expression level of ATM protein, but possibly by overall recombination activity with other modifier genes or with environmental factors other than infections. Moreover, 12 sibling pairs showed substantially different IgA levels. More detailed analysis of AT children with hypogammaglobulinemia will lead to better understanding of the involvement of ATM in V(D)J recombination and in CSR.

Finally, we evaluated whether the phenotypic variations were due to the mutation type or the age difference by comparing the phenotypes and laboratory data between the sibling pairs with the same ATM mutations. The data were accumulated at a similar age whenever possible.

Our study demonstrated some similarity and difference in the clinical phenotypes and a wide variety in the immunological parameters of the sibling pairs. Thus, it is not likely that the variations were due to age difference or ATM mutation type. The diverse phenotypes and immunological data of the sibling cases suggest a modifier gene(s) and environmental factor(s), or both also serve as important determinants of the patients' phenotypes.

Our data demonstrate that median age at diagnosis, onset of telangiectasia, and longevity were similar to those of previous reports [4, 5, 7]. The most common cause of death was infection, particularly lower respiratory infection at older ages. The proportion of AT patients who developed chorea, malignancy, diabetes mellitus, or short stature was not different from data previously reported.

This paper described the results of the first nationwide survey of AT patients in Japan. Despite the limitations associated with a retrospective study, our data shed light on important issues in AT patients. These data will lead to better patient care as well as understanding of pathogenesis and diverse phenotypes of AT children.

Acknowledgments This work was in part supported by grants from the Ministry of Health, Labour, and Welfare and from the Ministry of Education, Culture, Sports, Science, and Technology to SM and TM.

Conflict of interest statement We have no financial relationships or conflict of interest relevant to this manuscript to be disclosed.

References

1. Claret Teruel G, Giner Munoz MT, Plaza Martin AM, Martin Mateos MA, Piquer Gibert M, Sierra Martinez JI. Variability of immunodeficiency associated with ataxia telangiectasia and

clinical evolution in 12 affected patients. Pediatr Allergy Immunol. 2005;16:615–8.
2. Gatti RA. Ataxia-telangiectasia. In: Scriver CR, Beaudet AL, Sly WS, editors. Metabolic and molecular basis of inherited diseases. New York: Mcgraw-Hill; 2001. p. 1187–96.
3. Gatti RA, Becker-Catania S, Chun HH, Sun X, Mitui M, Lai CH, et al. The pathogenesis of ataxia-telangiectasia. Learning from a Rosetta Stone. Clin Rev Allergy Immunol. 2001;20:87–108.
4. Perlman S, Becker-Catania S, Gatti RA. Ataxia-telangiectasia: diagnosis and treatment. Semin Pediatr Neurol. 2003;10:173–82.
5. Cabana MD, Crawford TO, Winkelstein JA, Christensen JR, Lederman HM. Consequences of the delayed diagnosis of ataxia-telangiectasia. Pediatrics. 1998;102:98–100.
6. Moin M, Aghamohammadi A, Kouhi A, Tavassoli S, Rezaei N, Ghaffari SR, et al. Ataxia-telangiectasia in Iran: clinical and laboratory features of 104 patients. Pediatr Neurol. 2007;37:21–8.
7. Crawford TO, Skolasky RL, Fernandez R, Rosquist KJ, Lederman HM. Survival probability in ataxia telangiectasia. Arch Dis Child. 2006;91:610–1.
8. Nowak-Wegrzyn A, Crawford TO, Winkelstein JA, Carson KA, Lederman HM. Immunodeficiency and infections in ataxia-telangiectasia. J Pediatr. 2004;144:505–11.
9. Vacchio MS, Olaru A, Livak F, Hodes RJ. ATM deficiency impairs thymocyte maturation because of defective resolution of T cell receptor alpha locus coding end breaks. Proc Natl Acad Sci USA. 2007;104:6323–8.
10. Savitsky K, Bar-Shira A, Gilad S, Rotman G, Ziv Y, Vanagaite L, et al. A single ataxia telangiectasia gene with a product similar to PI-3 kinase. Science. 1995;268:1749–53.
11. Lange E, Borresen AL, Chen X, Chessa L, Chiplunkar S, Concannon P, et al. Localization of an ataxia-telangiectasia gene to an approximately 500-kb interval on chromosome 11q23.1: linkage analysis of 176 families by an international consortium. Am J Hum Genet. 1995;57:112–9.
12. Taylor AM, Byrd PJ. Molecular pathology of ataxia telangiectasia. J Clin Pathol. 2005;58:1009–15.
13. Shiloh Y. ATM and related protein kinases: safeguarding genome integrity. Nat Rev Cancer. 2003;3:155–68.
14. Shiloh Y. The ATM-mediated DNA-damage response: taking shape. Trends Biochem Sci. 2006;31:402–10.
15. Reliene R, Schiestl RH. Antioxidants suppress lymphoma and increase longevity in ATM-deficient mice. J Nutr. 2007;137:229S–32S.
16. Reliene R, Schiestl RH. Antioxidant *N*-acetyl cysteine reduces incidence and multiplicity of lymphoma in Atm deficient mice. DNA Repair (Amst). 2006;5:852–9.
17. Du L, Pollard JM, Gatti RA. Correction of prototypic ATM splicing mutations and aberrant ATM function with antisense morpholino oligonucleotides. Proc Natl Acad Sci USA. 2007;104:6007–12.
18. Lai CH, Chun HH, Nahas SA, Mitui M, Gamo KM, Du L, et al. Correction of ATM gene function by aminoglycoside-induced read-through of premature termination codons. Proc Natl Acad Sci USA. 2004;101:15676–81.
19. Oguchi K, Takagi M, Tsuchida R, Taya Y, Ito E, Isoyama K, et al. Missense mutation and defective function of ATM in a childhood acute leukemia patient with MLL gene rearrangement. Blood. 2003;101:3622–7.
20. Takagi M, Tsuchida R, Oguchi K, Shigeta T, Nakada S, Shimizu K, et al. Identification and characterization of polymorphic variations of the ataxia telangiectasia mutated (ATM) gene in childhood Hodgkin disease. Blood. 2004;103:283–90.
21. Gilad S, Chessa L, Khosravi R, Russell P, Galanty Y, Piane M, et al. Genotype-phenotype relationships in ataxia-telangiectasia and variants. Am J Hum Genet. 1998;62:551–61.
22. Birrell GW, Kneebone K, Nefedov M, Nefedova E, Jartsev MN, Mitsui M, et al. ATM mutations, haplotype analysis, and immunological status of Russian patients with ataxia telangiectasia. Hum Mutat. 2005;25:593.
23. Morio T, Hanissian S, Geha RS. Characterization of a 23-kDa protein associated with CD40. Proc Natl Acad Sci USA. 1995;92:11633–6.
24. Morio T, Hanissian SH, Bacharier LB, Teraoka H, Nonoyama S, Seki M, et al. Ku in the cytoplasm associates with CD40 in human B cells and translocates into the nucleus following incubation with IL-4 and anti-CD40 mAb. Immunity. 1999;11:339–48.
25. Morio T, Nagasawa M, Nonoyama S, Okawa H, Yata J. Phenotypic profile and functions of T cell receptor-gamma delta-bearing cells from patients with primary immunodeficiency syndrome. J Immunol. 1990;144:1270–5.
26. Al-Harthi L, Marchetti G, Steffens CM, Poulin J, Sekaly R, Landay A. Detection of T cell receptor circles (TRECs) as biomarkers for de novo T cell synthesis using a quantitative polymerase chain reaction-enzyme linked immunosorbent assay (PCR-ELISA). J Immunol Methods. 2000;237:187–97.
27. Suzuki K, Tsugawa K, Oki E, Morio T, Ito E, Tanaka H, et al. Vesical varices and telangiectasias in a patient with ataxia telangiectasia. Pediatric Nephrology. 2008;23:1005–8.
28. Giovannetti A, Mazzetta F, Caprini E, Aiuti A, Marziali M, Pierdominici M, et al. Skewed T-cell receptor repertoire, decreased thymic output, and predominance of terminally differentiated T cells in ataxia telangiectasia. Blood. 2002;100:4082–9.
29. Chun HH, Gatti RA. Ataxia-telangiectasia, an evolving phenotype. DNA Repair (Amst). 2004;3:1187–96.
30. Marshall FF, Klinefelter HF. Late hemorrhagic cystitis following low-dose cyclophosphamide therapy. Urology. 1979;14:573–5.
31. Stillwell TJ, Benson RC Jr. Cyclophosphamide-induced hemorrhagic cystitis. A review of 100 patients. Cancer. 1988;61:451–7.
32. Walker RD. Cyclophosphamide induced hemorrhagic cystitis. J Urol. 1999;161:1747.
33. Mizutani S. Genetic background as a possible determinant of clinical and biological features of Epstein-Barr virus infection—a hypothetical view. Crit Rev Oncol Hematol. 2002;44:217–25.
34. Pan Q, Petit-Frere C, Lahdesmaki A, Gregorek H, Chrzanowska KH, Hammarstrom L. Alternative end joining during switch recombination in patients with ataxia-telangiectasia. Eur J Immunol. 2002;32:1300–8.
35. Pan-Hammarstrom Q, Dai S, Zhao Y, van Dijk-Hard IF, Gatti RA, Borresen-Dale AL, et al. ATM is not required in somatic hypermutation of VH, but is involved in the introduction of mutations in the switch mu region. J Immunol. 2003;170:3707–16.
36. Pan-Hammarstrom Q, Lahdesmaki A, Zhao Y, Du L, Zhao Z, Wen S, et al. Disparate roles of ATR and ATM in immunoglobulin class switch recombination and somatic hypermutation. J Exp Med. 2006;203:99–110.
37. Peron S, Pan-Hammarstrom Q, Imai K, Du L, Taubenheim N, Sanal O, et al. A primary immunodeficiency characterized by defective immunoglobulin class switch recombination and impaired DNA repair. J Exp Med. 2007;204:1207–16.
38. Reina-San-Martin B, Chen J, Nussenzweig A, Nussenzweig MC. Enhanced intra-switch region recombination during immunoglobulin class switch recombination in 53BP1−/− B cells. Eur J Immunol. 2007;37:235–9.
39. Soresina A, Meini A, Lougaris V, Cattaneo G, Pellegrino S, Piane M, et al. Different clinical and immunological presentation of ataxia-telangiectasia within the same family. Neuropediatrics. 2008;39:43–5.

Immunologically silent cancer clone transmission from mother to offspring

Takeshi Isoda[a,1], Anthony M. Ford[b,1], Daisuke Tomizawa[a], Frederik W. van Delft[b], David Gonzalez De Castro[b], Norkio Mitsuiki[a], Joannah Score[c], Tomohiko Taki[d], Tomohiro Morio[a], Masatoshi Takagi[a], Hiroh Saji[e], Mel Greaves[b,2,3], and Shuki Mizutani[a,2,3]

[a]Department of Pediatrics and Developmental Biology, Tokyo Medical and Dental University, 1-5-45 Yushima, Bunkyo-ku, Tokyo 1138519, Japan; [b]Section of Haemato-Oncology, Institute of Cancer Research, Brookes Lawley Building, 15 Cotswold Road, Sutton, Surrey SM2 5NG, United Kingdom; [c]Wessex Regional Genetics Laboratory, University of Southampton, Salisbury District Hospital, Salisbury SP2 8BJ, United Kingdom; [d]Department of Molecular Laboratory Medicine, Kyoto Prefectural University of Medicine Graduate School of Medical Science, 465 Kajii Cho, Hirokoji-agaru, Kawaramachi, Kamigyo-ku, Kyoto 6028566, Japan; and [e]Human Leukocyte Antigen Laboratory, Ebis Building, 3-4F, 82 Shimo-Tsutsumimachi, Marutamachi-kudaru, Kawabata Dori, Sakyo-ku, Kyoto 606-8396, Japan

Edited by Janet D. Rowley, University of Chicago Medical Center, Chicago, IL, and approved July 28, 2009 (received for review April 28, 2009)

Rare cases of possible materno-fetal transmission of cancer have been recorded over the past 100 years but evidence for a shared cancer clone has been very limited. We provide genetic evidence for mother to offspring transmission, in utero, of a leukemic cell clone. Maternal and infant cancer clones shared the same unique *BCR-ABL1* genomic fusion sequence, indicating a shared, single-cell origin. Microsatellite markers in the infant cancer were all of maternal origin. Additionally, the infant, maternally-derived cancer cells had a major deletion on one copy of chromosome 6p that included deletion of HLA alleles that were not inherited by the infant (i.e., foreign to the infant), suggesting a possible mechanism for immune evasion.

fetus | fusion gene | leukemia

Rare cases of melanoma or hemopoietic malignancies in infants have been recorded that may have been of maternal origin (1). Genetic evidence for a shared, materno-fetal clone of cancer cells has, however, to date, been sparse and based upon limited karotype information (1). Unambiguous attribution of transmission of a cancer clone should be achievable by genetic fingerprinting, the most striking precedent for which is canine transmissible venereal sarcoma (CTVS) in which multiple cases worldwide derive from a single clone (2). Leukemia fusion genes, generated by chromosome translocations, have patient-specific or idiosyncratic genomic sequences at the fusion breakpoints and are frequently early or initiating events (3). They therefore provide stable, specific, and sensitive clonal markers and can unambiguously identify a single-cell origin in different individuals as documented with monozygotic twins with concordant leukemia (4). We report here equivalent genetic scrutiny of a case of concordant maternal and infant ALL/lymphoma with the *BCR-ABL1* fusion gene.

Results

The Mother. The Japanese mother was 28 years old at her child's delivery. No hematological abnormalities had been identified during the pregnancy, and the birth was uncomplicated. Thirty-six days after the delivery, the mother experienced vaginal bleeding. On day 39, she developed fever, and on day 43, bleeding became uncontrollable. Blood showed leukocytosis (206,800/μL) with 97% lymphoblasts, anemia (hemoglobin level: 3.5g/dL), and thrombocytopenia (platelet count: $0.2 \times 10^4/\mu$L). Bone marrow aspiration revealed peroxidase-negative lymphoblasts (99.6% of nucleated cells), which were positive for CD10, CD19, CD20, CD34, TdT, and CD79a. Chromosomal G-banding showed 46,XX,t (9, 22)(q34;q11), and 3.2×10^5 copies/μgRNA of p190-type *BCR-ABL1* mRNA were detected by RT-PCR. She was diagnosed as having B-cell precursor Ph+ ALL (see *SI Text* for clinical treatment).

The Infant. The 11-month-old female offspring of the above mother was admitted to hospital with right cheek swelling. MRI revealed a mass in the cheek (Fig. S1*A*) and a pleural effusion of the lung. There was no lymph node swelling or organomegaly. She was born with normal delivery at 40 weeks, 5 days gestation. There was no history of prenatal abnormalities including intrauterine growth retardation, and she showed normal growth and development until admission.

Laboratory Findings on Infant Samples. Laboratory analyses of the maternal and infant samples was carried out with full ethical approval in accordance with the Declaration of Helsinki (Local ethics approval # CCR2285) and with informed consent of the family (father). Biopsy of the primary jaw tumor showed the presence of small round blue cell tumor with large nucleus/cytoplasm ratio, which diffusely proliferated with partial hyalinization of stroma. A large antibody panel was used to distinguish a sarcoma from lymphoma. LCA, CD10, CD20, CD79a, TdT, CD34, and MIC2 were positive by immunohistochemical staining, and CD3, CD5, CD56, desmin, HHF35, S100, GFAP, chromogranin, and synaptophysin were all negative. No cytogenetic analysis was performed but subsequent FISH analysis revealed positivity for the *BCR-ABL1* gene (Fig. S1*B*).

Cells (48.2%) in the pleural fluid were positive for CD10, CD19, CD34, and HLA-DR and p190-type *BCR-ABL1* chimeric mRNA was detected (9.5×10^4 copies/μgRNA) by quantitative RT-PCR (Q-PCR).

Blood count findings on the infant were as follows; WBC 10,100/μL (segment forms 22%; lymphocytes 72%; monocytes 5%; eosinophil 1%), hemoglobin level 12.5 g/dL, platelet count $38.4 \times 10^4/\mu$L. No blast cells were detected in the cerebrospinal fluid, and there was no morphological evidence of tumor infiltration in bone marrow. Bone marrow aspirates were negative for *BCR-ABL1* chimeric mRNA by Q-PCR. The patient's neoplastic cells had the same immunophenotype and abnormal genotype (*BCR-ABL1* fusion) as her mother's ALL but, in light of the presentation features, she was diagnosed as having B-cell precursor lymphoblastic lymphoma stage III by the St. Jude Staging System (see *SI Text* for clinical treatment of infant).

Author contributions: M.G. and S.M. designed research; A.M.F., D.T., F.W.v.D., D.G.D.C., N.M., J.S., T.T., T.M., M.T., and H.S. performed research; T.I. contributed new reagents/analytic tools; M.G. and S.M. analyzed data; and M.G. and S.M. wrote the paper.

The authors declare no conflict of interest.

This article is a PNAS Direct Submission.

[1]T.I. and A.M.F. contributed equally to this work.

[2]M.G. and S.M. contributed equally to this work.

[3]To whom correspondence may be addressed. E-mail: mel.greaves@icr.ac.uk or skkm12@gmail.com.

This article contains supporting information online at www.pnas.org/cgi/content/full/0904658106/DCSupplemental.

www.pnas.org/cgi/doi/10.1073/pnas.0904658106

Impaired CD4 and CD8 Effector Function and Decreased Memory T Cell Populations in ICOS-Deficient Patients

Naomi Takahashi,* Kenji Matsumoto,† Hirohisa Saito,† Toshihiro Nanki,‡ Nobuyuki Miyasaka,‡ Tetsuji Kobata,§ Miyuki Azuma,¶ Sang-Kyou Lee,‖ Shuki Mizutani,* and Tomohiro Morio[1]*

Interaction of ICOS with its ligand is essential for germinal center formation, T cell immune responses, and development of autoimmune diseases. Human ICOS deficiency has been identified worldwide in nine patients with identical ICOS mutations. In vitro studies of the patients to date have shown only mild T cell defect. In this study, we report an in-depth analysis of T cell function in two siblings with novel ICOS deficiency. The brother displayed mild skin infections and impaired Ig class switching, whereas the sister had more severe symptoms, including immunodeficiency, rheumatoid arthritis, inflammatory bowel disease, interstitial pneumonitis, and psoriasis. Despite normal CD3/CD28-induced proliferation and IL-2 production in vitro, peripheral blood T cells in both patients showed a decreased percentage of CD4 central and effector memory T cells and impaired production of Th1, Th2, and Th17 cytokines upon CD3/CD28 costimulation or PMA/ionophore stimulation. The defective polarization into effector cells was associated with impaired induction of T-bet, GATA3, MAF, and retinoic acid-related orphan nuclear hormone receptor (RORC). Reduced CTLA-4$^+$CD45RO$^+$FoxP3$^+$ regulatory T cells and diminished induction of inhibitory cell surface molecules, including CTLA-4, were also observed in the patients. T cell defect was not restricted to CD4 T cells because reduced memory T cells and impaired IFN-γ production were also noted in CD8 T cells. Further analysis of the patients demonstrated increased induction of receptor activator of NF-κB ligand (RANKL), lack of IFN-γ response, and loss of Itch expression upon activation in the female patient, who had autoimmunity. Our study suggests that extensive T cell dysfunction, decreased memory T cell compartment, and imbalance between effector and regulatory cells in ICOS-deficient patients may underlie their immunodeficiency and/or autoimmunity. *The Journal of Immunology,* **2009, 182: 5515–5527.**

Members of the CD28 family play an important role in the regulation of T cell immune responses (1, 2). Expression of these molecules and their ligands is tightly regulated to deliver either costimulatory or inhibitory signals (2–5), and their uncoordinated regulation leads to the development of immunological disorders (6–8).

ICOS (CD278) is a costimulatory member of the CD28 family, and its expression is induced in CD4 T cells upon activation (9–11). The ICOS signal is induced by interaction with its partner, the ICOS ligand (ICOS-L[2]; CD275), a molecule highly expressed on B cells and dendritic cells and weakly on T cells and nonlymphoid cells (1, 12). Signaling through ICOS enhances T cell proliferation, secretion of cytokines, and up-regulation of cell surface molecules (11, 13, 14).

Previous research has showed that the ICOS-ICOS-L interaction is important for productive T-B cell coactivation, CD40-mediated Ig class switch recombination, and development of Th2 immune responses (1, 15–17). Induction of the Th1 cytokine IFN-γ is relatively unaffected and in some studies augmented; other studies have documented the importance of ICOS in Th1 responses (15, 16, 18–21). Accumulating evidence indicates that ICOS also regulates the generation of Th17 cells, differentiation of FoxP3$^+$ regulatory T cells (Tregs), and homeostatic survival of invariant NKT (iNKT) cells (22–24).

Although earlier investigations of ICOS-null mice revealed normal numbers of naive/memory T cells and normal primary clonal expansion and survival of memory T cells, more recent investigation has demonstrated lower numbers of effector memory T cells (TEMs) in ICOS$^{-/-}$ mice in the steady state (23). Seemingly contradictory results have been reported on the requirement of ICOS for T cell differentiation and function.

Most studies have depicted ICOS as a costimulator. Indeed, the blockade of the ICOS-ICOS-L interaction abrogates the development of murine models of autoimmune diseases, as follows: rheumatoid arthritis (RA), inflammatory bowel disease (IBD), myasthenia gravis, type I diabetes mellitus, experimental myositis, autoimmune carditis, and graft-vs-host disease (25–30).

Previously, human ICOS deficiency has been reported in nine patients from four families (31–33). Importantly, the same homologous genetic deletion of exons 2 and 3 was identified in all patients, indicating a founder effect in all four families. Analysis of these patients revealed reduced numbers of memory B cells and pan-hypoimmunoglobulinemia, but no impairment in the secretion of TNF-α, IFN-γ, IL-2, IL-4, IL-10, or IL-13. Normal surface

*Department of Pediatrics and Developmental Biology, Graduate School of Medical and Dental Sciences, Tokyo Medical and Dental University, Tokyo, Japan; †Department of Allergy and Immunology, National Research Institute for Child Health and Development, Tokyo, Japan; ‡Department of Medicine and Rheumatology, Graduate School of Medical and Dental Sciences, Tokyo Medical and Dental University, Tokyo, Japan; §Department of Immunology, Dokkyo Medical University, Tochigi, Japan; ¶Department of Molecular Immunology, Graduate School of Medical and Dental Sciences, Tokyo Medical and Dental University, Tokyo, Japan; and ‖Department of Biotechnology, Yonsei University, Seoul, Korea

Received for publication October 6, 2008. Accepted for publication February 24, 2009.

The costs of publication of this article were defrayed in part by the payment of page charges. This article must therefore be hereby marked *advertisement* in accordance with 18 U.S.C. Section 1734 solely to indicate this fact.

[1] Address correspondence and reprint requests to Dr. Tomohiro Morio, Tokyo Medical and Dental University Graduate School of Medicine, 1-5-45 Yushima, Bunkyo-Ku, Tokyo 113-8519, Japan. E-mail address: tmorio.ped@tmd.ac.jp

[2] Abbreviations used in this paper: ICOS-L, ICOS ligand; IBD, inflammatory bowel disease; IP, interstitial pneumonitis; RA, rheumatoid arthritis; RE, relative expression; TCM, central memory T cell; TEM, effector memory T cell; Treg, regulatory T cell; BTLA, B and T lymphocyte attenuator; EOMES, eomesodermin; PD-1, programmed death-1; RANKL, receptor activator of NF-κB ligand; RORC, retinoic acid-related orphan nuclear hormone receptor.

www.jimmunol.org/cgi/doi/10.4049/jimmunol.0803256

expression of CD69, CD40L (CD154), CD25, and OX40 (CD134) was observed on their T cells following stimulation (31). A later study provided evidence of defects in IL-10 and IL-17 production (33); however, no major impairment of T cell function was demonstrated. Autoimmunity, manifested as autoantibody-mediated neutropenia, was observed in only one patient (33). Although there have been reports on the effects of ICOS on CD8 responses in mice (34, 35), impact of ICOS on CD8 T cells is not yet completely understood.

In this study, we describe the case of two siblings having ICOS deficiency with a novel mutation in the ICOS gene. Although both patients displayed varing degrees of immunodeficiency, only the sister showed a wide range of autoimmune diseases, including RA, IBD, interstitial pneumonitis (IP), and psoriasis.

In this study, we focused on the T cell immune function of these ICOS-deficient patients. Detailed analysis demonstrated a reduction in memory T cells and a major subtype of Tregs; impaired polarization into Th1, Th2, and Th17; and defective induction of CTLA-4 molecules and other surface inhibitory receptors.

We further assessed activation-induced T cell proliferation and apoptosis, induction of costimulatory receptor molecules, and expression of master regulators for effector T cell subsets, and explored the mechanisms of T cell defect and autoimmunity in these patients using quantitative mRNA analysis.

Materials and Methods

Patients and controls

Patients were diagnosed with common variable immunodeficiency, according to the European Society for Immunodeficiencies criteria (www.esid.org). Twelve healthy volunteers (6 male, 6 female) aged between 26 and 48 years were recruited. The study was approved by the institutional ethical committee of Tokyo Medical and Dental University, and written informed consent was obtained from the patients, the elder sister and mother of the patients, and healthy controls.

Sequencing and RT-PCR of ICOS

Genomic DNA was extracted from peripheral blood using a DNA blood mini kit (Qiagen), according to the manufacturer's instructions. The coding sequences of the five exons and the adjacent intron-exon boundaries of the ICOS gene were amplified with specific primers (sequences are available upon request) from genomic DNA on the basis of ICOS sequences obtained from GenBank database (accession numbers AC103880, AC009965, and AB023135). All PCR products were sequenced using BigDye terminator v3.1 and an ABI Prism 3130 Genetic Analyzer (Applied Biosystems); the sequence data were then analyzed using DNASIS software (Hitachi Software). Total RNA was isolated from stimulated PBMCs using an RNeasy mini kit (Qiagen) and reverse transcribed into cDNA using a Superscript III first-strand synthesis system for RT-PCR (Invitrogen). PCR products were separated by agarose gel electrophoresis.

Monoclonal Abs

We used the following FITC-, PE-, PE Texas Red (ECD)-, or PE cyanin 5.1 (PC5)-conjugated Abs: FoxP3 (236A/E7) from Abcam; IgG1 isotype controls, CD3 FITC, CD3 PE (SK7), CD4 PE (SK3), CD8 FITC, CD8 PE (SK1), CD25 FITC (M-A251), IL-4 PE (3010.211), IFN-γ PE (25723.11), 4-1BB PE (4B4-1), OX40 PE (ACT35), and IL-10 PE (JES3-10F1) from BD Pharmingen; CD3 FITC (UCHT1), CD4 PC5 (13B8.2), CD8 ECD (SFCI21Thy2D3), CD8 FITC (B9.11), CD19 ECD, CD19 PE (J4.119), CD20 FITC (B9E9), CD25 PC5 (B1.49.1), CD28 FITC, CD28 purified (CD28.2), CD45RA FITC (ALB11 and 2H4), CD45RO PE, ECD (UCHL1), CD62L ECD (DREG56), CD69 PE (TP1.55.3), CTLA4 PE (BNI3), streptavidin FITC, streptavidin PC5, and TCR Vβ Repertoire kit from Beckman Coulter (CA); CD27 PE (M-T271) and IgD from Dako-Cytomation; CD45RO PE (UCHL1), IL-17 FITC (eBio64DEC17), B and T lymphocyte attenuator (BTLA) PE (MIH26), programmed death-1 (PD-1) FITC (MIH4), ICOS-L, ICOSL biotin (MIH12), and ICOS FITC (ISA-3) from eBioscience; receptor activator of NF-κB (RANK) PE (9A725) from Imgenex; CD25 PE (4E3) from Miltenyi Biotec; Alexa Fluor 488 goat anti-mouse IgG Ab from Molecular Probes; CCR7 FITC (150503) from eBioscience; and CD3 purified (OKT3) from Janssen Pharmaceutical.

Cell separation and stimulation

PBMCs were isolated from heparinized blood using Lymphoprep (Axis-Shield), as described previously (36). CD4 T cells were negatively selected from the PBMCs using a StemSep device (StemCell Technologies). Thus, the purity of the collected CD4 T cell population was generally >95%. CD8 T cells were prepared with the same technique yielding >90% pure CD8 T cell population. Separated cells were resuspended in RPMI 1640 (WAKO) supplemented with 10% heat-inactivated FBS (Gemini Biological Products), and incubated at 10^6 cells/ml in 24-well plates (Greiner Bioscience) with or without stimulants. For stimulation, we used anti-CD28 mAb (at 1 μg/ml) with plate-bound anti-CD3 mAb or 50 ng/ml PMA (Sigma-Aldrich) plus 1 μg/ml ionomycin (Sigma-Aldrich). The cells were incubated in the medium at 37°C in 5% CO_2 for the indicated time periods. IL-2 (Lymphotec) was used at 700 IU/ml with plate-bound anti-CD3 when assessing ICOS expression.

Flow cytometric analysis

PBMCs, CD4 T cells, or CD8 T cells were stained with the indicated Abs and were analyzed using a FACSCalibur flow cytometer and CellQuest software (BD Biosciences) or an EPICS XL flow cytometer and EXPO32 software (Beckman Coulter), as described previously (37). For intracellular cytokine detection, PBMCs were stimulated with PMA and ionomycin in the presence of GolgiPlug (BD Pharmingen) or brefeldin A (eBioscience) for 5–8 h at 37°C in 5% CO_2. After stimulation, the cells were fixed and permeabilized using a Cytofix/Cytoperm Plus fixation/permeabilization kit (BD Pharmingen). The same permeabilization technique was used to detect CTLA-4 expression. A CellTrace CFSE cell proliferation kit (Molecular Probes) was used for the CFSE assay, and an annexin V FITC/7-AAD kit (Beckman Coulter) for the apoptosis assay.

Cytokine production assay

Negatively selected CD4 T cells or CD8 T cells were incubated with or without stimulants (plate-bound anti-CD3 mAb and anti-CD28 mAb or 50 ng/ml PMA, and 200 nM ionomycin). The supernatants were collected after 24 h and analyzed using ELISA for IL-17, IL-12p40, IL-22, and TGF-β1 (R&D Systems); IL-21 (eBioscience); and human Th1/Th2 cytokines (IFN-γ, IL-2, IL-4, IL-5, IL-6, IL-10, TNF-α, and TNF-β) using a FlowCytomix kit (Bender MedSystems), according to the manufacturer's instructions. All assays were performed in duplicate.

Real-time quantitative PCR

Total RNA was extracted using an RNeasy mini kit with DNase (Qiagen) and reverse transcribed using random hexamer primers and Superscript III reverse transcriptase (Invitrogen). Real-time quantitative PCR was performed using a 7300 Real-Time PCR system (Applied Biosystems) using an assay-on-demand Taqman probe and primers (Hs00174383 for *IL17A*, Hs00243522 for *RANKL*, Hs00203958 for *FOXP3*, Hs00226053 for *RNF128*, Hs00909784 for *CBLB*, Hs00395208 for *ITCH*, Hs00172872 for *EOMES*, Hs00193519 for *MAF*, Hs00231122 for *GATA3*, Hs00894392 for *TBX21*, Hs01076112 for *RORC*, Hs99999901 for *18S*, and Hs99999905 for *GAPDH*), according to the manufacturer's instructions. Relative expression levels of these genes were normalized according to *GAPDH* or *18S rRNA* expression, using a standard curve method as described by the manufacturer. All samples and standards were tested in duplicate.

Oligonucleotide microarray assay

Oligonucleotide microarray assay was conducted with total RNA extracted from a total of 1–3 × 10^6 CD4 T cells stimulated in anti-CD3-coated plates in the presence of anti-CD28 mAb or from unstimulated CD4 T cells, as described previously (38). Data analysis, selection of significant signals, and comparison of the data from multiple samples were conducted, as previously described (38). The results have been deposited in the Gene Expression Omnibus at http://www.ncbi.nlm.nih.gov/geo/(accession number GSE12875).

Results

Clinical course of patients and diagnosis of ICOS deficiency

The sister, hereafter designated patient 1, was born in 1967. In her infancy, she had episodes of prolonged viral infection. In 2001, when she developed a pulmonary abscess following appendectomy, she was diagnosed with common variable immunodeficiency according to the European Society for Immunodeficiencies criteria (at the age of 34), and i.v. Ig treatment was started to

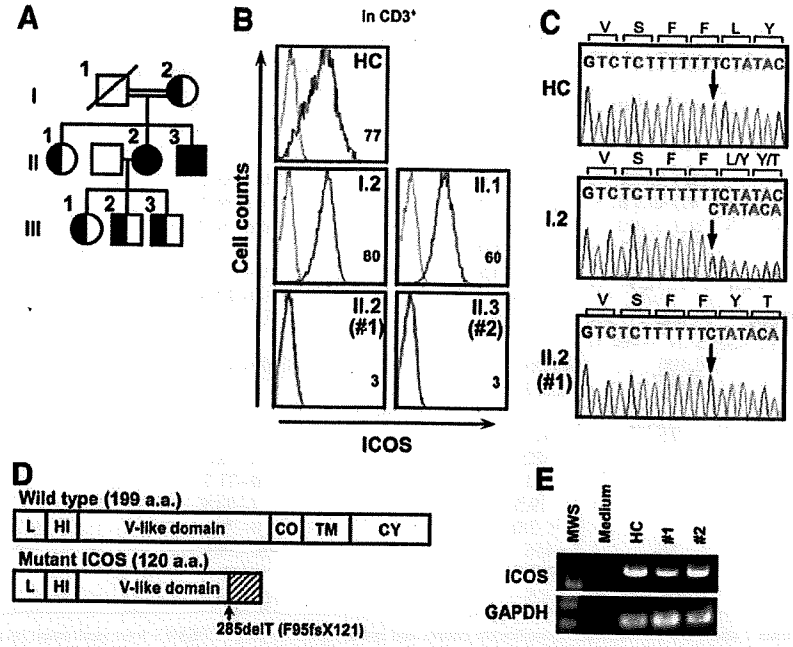

FIGURE 1. Diagnosis of ICOS deficiency. *A*, Pedigree of the ICOS deficiency patients. Filled symbols represent affected family members (II.2, patient 1; II.3, patient 2). The patients were products of a consanguineous marriage. *B*, Expression of ICOS. PBMCs from patients 1 and 2, their mother (I.2), elder sister (II.1), and a healthy control (HC) were cultured on an anti-CD3 mAb-coated plate in the presence of IL-2 and stained with anti-ICOS mAb (solid line) or control mAb (dotted line). The graphs are gated on CD3 T cells. Mean fluorescence intensity of ICOS is shown in each graph. *C*, Partial sequences of exon 2 of *ICOS* from HC, the mother of the patients, and patient 1. The elder sister of the patients had a heterozygous mutation that was detected in the mother, and the brother (patient 2) had a homozygous mutation at codon 285. *D*, Schematic figure showing the wild-type 199-aa ICOS protein and putative 120-aa mutant ICOS protein obtained from the patients. The shaded area represents the mutant proteins generated by induction of a frameshift at codon 285. L, L region; HI, hydrophilic region; CO, connecting region; TM, transmembrane region; CY, cytoplasmic region. *E*, RT-PCR analysis for *ICOS* mRNA. *ICOS* mRNA (1–597) from anti-CD3/IL-2-stimulated PBMCs from patient 1 (#1) and patient 2 (#2), and HC was amplified by RT-PCR with specific primers. The PCR product was analyzed by agarose gel electrophoresis. MWS, m.w. standard.

maintain the trough IgG level of >4 g/L. In the following years, she developed psoriasis-like cutaneous lesions and arthritis in multiple joints, including bilateral shoulder, wrist, knee, metacarpophalangeal, proximal interphalangeal, and metatarsophalangeal joints. RA was diagnosed on the basis of the findings of proliferative synovitis of multiple finger and toe joints with erosive changes on x-ray examination. Psoriatic arthritis was ruled out based on the joints affected and the x-ray findings. In 2003, she developed abdominal colic, diarrhea, and IP, and had a constantly elevated serum CRP level. Diagnosis of IBD was made upon biopsy of the colon, and both IBD and IP were controlled by prednisolone. She was referred to our hospital in 2006. Methotrexate at 8 mg/week significantly improved not only the articular signs and symptoms of RA, but also the psoriatic skin changes and IBD. The dose of prednisolone was successfully tapered from 15 to 8 mg/day. Since then, she has been on regular Ig supplementation every 2 wk.

The pedigree of the patient is shown in Fig. 1*A*. The patient had two siblings: her sister was healthy with no immunological abnormalities, whereas her younger brother (hereafter designated patient 2) developed occasional skin abscesses and mild psoriasis-like cutaneous lesions, and had slightly low levels of IgG (611 mg/dL) when examined at the age of 35. The serum IgG level stays at the same level to date; and he is not yet on Ig supplementation.

A summary of the immunological data of patients 1 and 2, the elder sister, and ICOS deficiency patients reported to date (33) is given in Table I. Patient 1 had a slightly reduced B cell count, whereas patient 2 had a normal B cell count. In both siblings, however, $CD27^+IgD^-$-switched memory B cells were virtually absent in the peripheral blood samples (Table I). The serum samples contained no detectable specific IgG Abs against measles, mumps, or rubella viruses despite a previous record of vaccine inoculation (data not shown). The immunological parameters of patient 2 are unique in that he showed elevated serum IgM (456 mg/dL). The T cells of the patients displayed abundant expression of CD69 and HLA-DR when stimulated via TCRs in the presence of exogenous IL-2 (data not shown), but lacked surface ICOS expression (Fig. 1*B*). Activated T cells from the mother (I.2) and elder sister (II.1) displayed normal ICOS induction.

Sequencing of the ICOS gene revealed the homozygous deletion of T at codon 285, which caused a frameshift in the coding region of ICOS and introduced a premature stop codon at aa 121 (F95fsX121) in the patients (Fig. 1, *C* and *D*).

Sequencing analysis of the *ICOS* gene in the elder sister and mother demonstrated a heterozygous mutation (Fig. 1*C*). RT-PCR of *ICOS* mRNA with specific primers amplifying the entire coding region of the *ICOS* gene (1–597) demonstrated the presence of an *ICOS* transcript, suggesting the absence of nonsense-mediated RNA decay (Fig. 1*E*).

Decreased memory T cells in ICOS-deficient patients

A previous report on human ICOS-deficient patients showed a normal distribution of naive, memory, and effector T cells (31, 33, 39). However, as seen in the representative FACS plots in Fig. 2*A*, we observed a substantial reduction in $CD4^+CD45RO^+$ memory cells in the patients compared with age- and gender-matched controls (12.1 and 6.6% for patients 1 and 2, respectively, and 24.5

Table 1. *Summary of immunological data*[a]

	Patient 1	Patient 2	Previously Reported ICOS-Deficient Patients (range)	II.1 (hetero)	Normal Range
Lymphocytes (/mm^3)	1,400 ± 200	1,900 ± 200	353–4,153	1,400	1,200–2,800
Immunophenotype of PBMCs (%)					
CD3	80.5 ± 5.0	72.4 ± 2.0	70.4–95.6	71.7	58–84
CD4	59.5 ± 5.0	55.6 ± 3.0	23.1–59.2	50.5	25–58
CD8	24.1 ± 4.0	19.1 ± 3.0	16.6–64.0	22.5	18–46
CD16	7.8 ± 0.2	11.2 ± 2.0	–	14.5	6–25
CD19	2.1 ± 0.6	4.8 ± 0.5	0.6–21.2	9.7	3–20
CD19$^+$CD27$^+$(%Bc)	0.2	0.8	2.0–12.6	11.4	8–35
CD19$^+$CD27$^+$IgD$^-$(%Bc)	0	0.4	0.0–1.3	8.6	7–32
Blastogenesis (cpm)					
PHA	56,100	45,600	78,900–95,700	–	20,500–56,800
Con A	45,300	32,500	–	–	20,300–65,700
Igs					
IgG (mg/dL)	315	611		1,025	900–1,600
IgG1	–	322	2.8–181	–	
IgG2	–	365	10–71.7	–	
IgG3	–	19.5	4–44.9	–	
IgG4	–	< 3.0	0–7	–	
IgM (mg/dL)	56	456	20–180	143	40–250
IgA (mg/dL)	46	103	6–58	137	100–250
IgE (IU/L)	<5	<5	17.5–38	ND	<173

[a] Immunological data of patients 1 and 2 are summarized. Lymphocyte counts and immunophenotyping of PBMCs were performed on more than three separate occasions; these are expressed as mean ± SD. Ig levels shown are those obtained at diagnosis (before Ig supplementation). Data from previous reported ICOS deficiency (33) and data from the elder sister of the patients are also shown. %Bc: % in B cells.

and 28.9% for controls 1 and 2, respectively). This reduction was seemingly counterbalanced by an increased frequency of naive T cells.

Gated CD4 memory T cells from PBMCs were further analyzed for CCR7 and CD62L expression to define CCR7$^+$-CD62L$^+$CD45RO$^+$ central memory T cells (TCMs) and

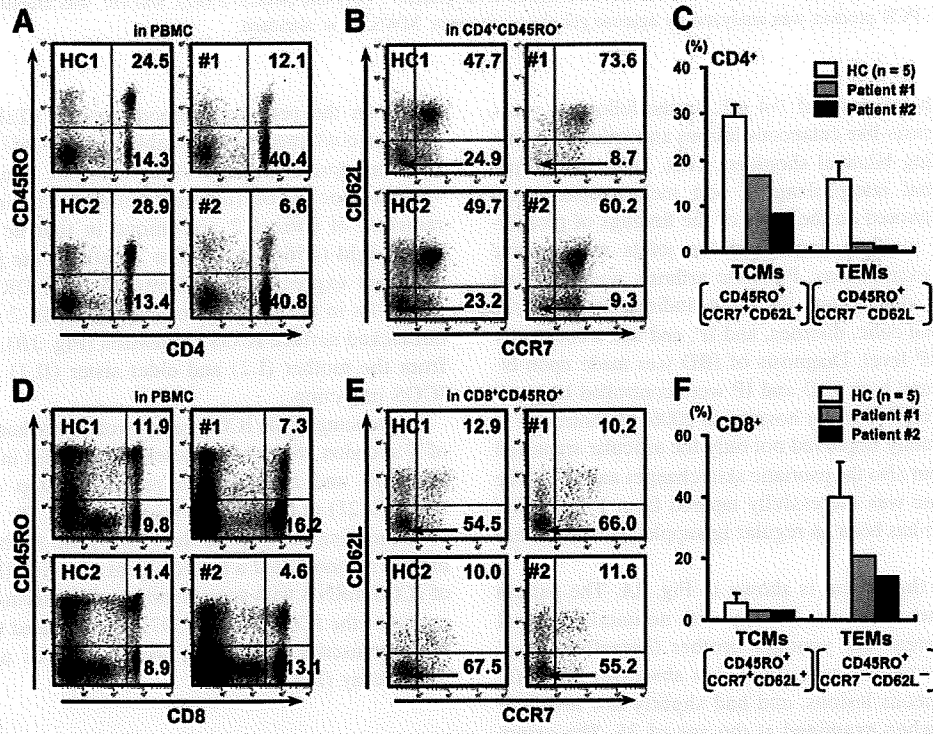

FIGURE 2. Decrease in memory T cells in ICOS-deficient patients. PBMCs from healthy controls (HC) and ICOS-deficient patients (1 and 2) were analyzed for the frequency of memory T cells. PBMCs were stained with Abs to CD4 or CD8, CD45RO, CCR7, and CD62L to assess memory T cell subsets (*A–F*). *A* and *D*, Representative CD4/CD45RO (*A*) and CD8/CD45RO (*D*) dot blots. Values shown in *upper* and *lower right quadrants* indicate percentages of the cells among total PBMCs. *B* and *E*, TCMs (CCR7$^+$CD62L$^+$) and TEMs (CCR7$^-$CD62L$^-$) in the memory CD4 T cell fraction (*B*) and in the memory CD8 T cell fraction (*E*). Values indicate frequencies of TCMs and TEMs in the CD4$^+$CD45RO$^+$ population or in the CD8$^+$CD45RO$^+$ population. Representative FACS analyses for healthy controls (HC) and patients are shown. *C* and *F*, Summary of percentages of TCMs and TEMs among CD4 T cells (*C*) and CD8 T cells (*F*). A □ with error bar represents the mean ± SD values of the indicated subsets from five healthy controls. Mean percentage for the respective subsets from two independent experiments is shown for the patients.

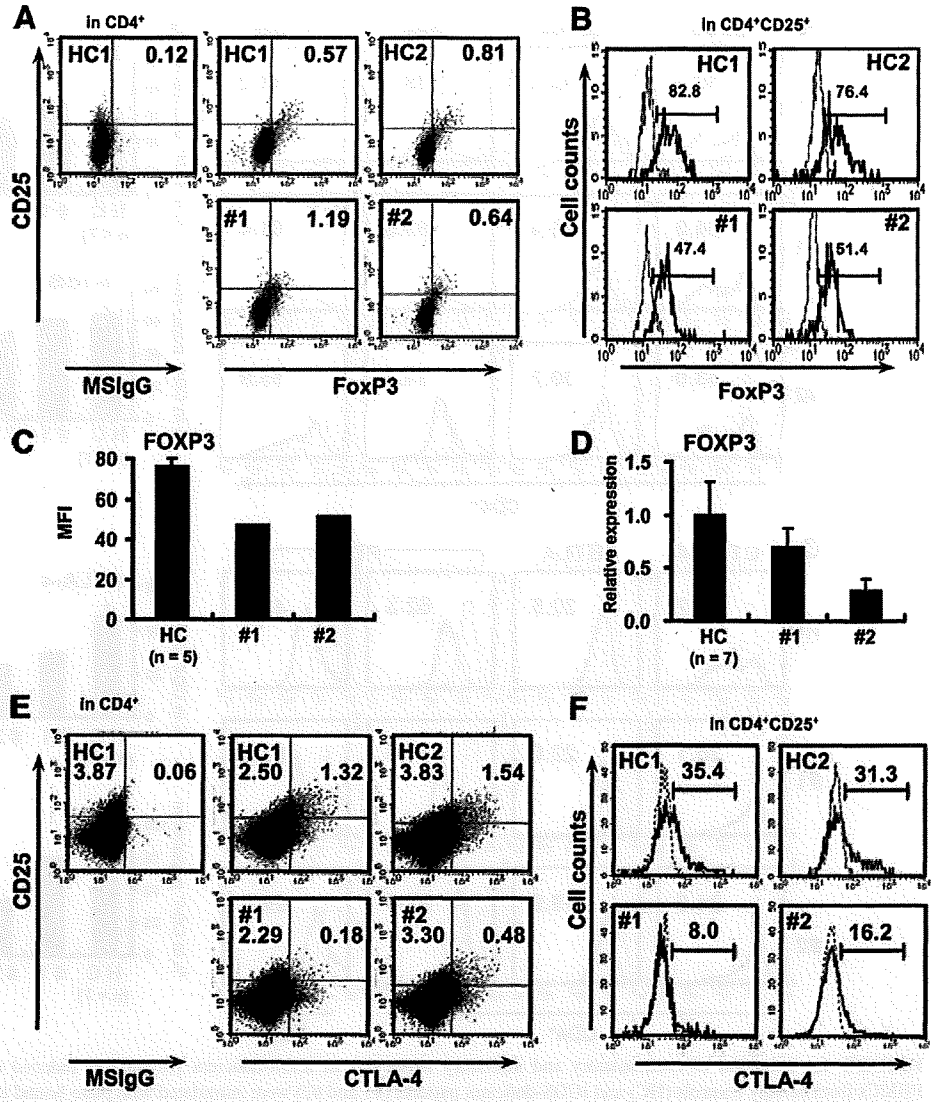

FIGURE 3. Decrease in CTLA-4$^+$ Treg subset in ICOS-deficient patients. *A*, Flow cytometric analysis of intracellular Foxp3 expression in CD4$^+$CD25$^+$ T cells. Numbers in dot plots are percentages of CD25$^+$-Foxp3$^+$ cells among CD4$^+$ T cells. *B*, Mean fluorescence intensity (MFI) of FoxP3 in CD4$^+$CD25$^+$ cells. FoxP3 expression in CD4$^+$CD25$^+$ cells is shown as a contour plot. MFI of FoxP3 is shown in the *upper right quadrant*. *C*, Summary of MFI of FoxP3 in CD4$^+$CD25$^+$ cells. *D*, Quantitative real-time PCR analysis for FoxP3 gene expression. mRNA expression levels in purified CD4 T cells were calculated with 18S rRNA as a reference, and the relative expression in healthy controls (HC) was adjusted to 1.0. Error bar indicates SD for HC and SEM for patients 1 and 2. *E* and *F*, Expression of CTLA-4 Ag in CD4$^+$CD25$^+$ T cells. Numbers indicate frequencies of CTLA-4$^+$ and CTLA-4$^-$ Treg subsets among CD4$^+$ T cells. PBMCs from five HC were analyzed by FACS. FACS analysis was performed three times for the patients. Representative dot plots (*E*) and contour plots (*F*) are shown. MFI of CTLA-4 in CD4$^+$CD25$^+$ Treg cells is indicated in the plots (*F*).

CCR7$^-$CD62L$^-$CD45RO$^+$ TEMs (40). The analysis showed that compared with controls, the patients had 2- to 5-fold fewer TCMs. The reduction in TEMs was more pronounced, with more than 6-fold fewer TEMs in the patients (Fig. 2, *B* and *C*).

A decrease in memory T cells was also observed in CD8 T cells. We observed a reduction in both TCMs and TEMs in patients compared with control subjects (n = 5) (Fig. 2, *D–F*).

Decreased Tregs in ICOS-deficient patients

Most Tregs express ICOS, and ICOS^{high+} Tregs preferentially produce IL-10 (41). In addition, recent studies have demonstrated the importance of ICOS in proliferation and maintenance of the pool size of FoxP3$^+$ Tregs (41). We therefore investigated the frequency of Treg cells in the two patients by staining their PBMCs for CD4, CD25, and intracellular FoxP3. Contrary to our predictions, the patients had a normal proportion of CD4$^+$CD25$^+$FoxP3$^+$ Tregs (Fig. 3*A*). However, we noted that the expression level of FoxP3, as reflected by the mean fluorescence intensity, was diminished in both patients (Fig. 3, *B* and *C*). To ascertain the low FoxP3 expression obtained in the FACS analysis, we evaluated the level of FoxP3 mRNA in a real-time PCR assay. This showed a marked reduction in FoxP3 expression in patient 2 and a slight decrease in patient 1 compared with the normal subjects (n = 7) (Fig. 3*D*).

Recent studies have shown that human CD4$^+$CD25$^+$FoxP3$^+$ Tregs comprise two subsets, as follows: IL-10-producing ICOS$^+$ CD45RO$^+$CTLA-4$^+$ Tregs and TGF-β-producing ICOS$^-$ CD45RA$^+$CTLA-4^{dull+} Tregs (42). This prompted us to examine CTLA-4 and CD45RO expression in the Tregs of ICOS-deficient patients. Fig. 3, *E* and *F*, demonstrates that most CD4$^+$CD25$^+$ Tregs in these patients were of the CTLA-4^{dull+} or CTLA-4$^-$ subpopulation and expressed CD45RA (data not shown), indicating that the CTLA-4$^+$ subset of Tregs that potentially produces IL-10 was severely decreased.

Defective induction of inhibitory molecules in ICOS-deficient patients

ICOS-null mice showed defective CD40-mediated Ig class switching because of lack of effective CD40L (CD154) up-regulation (15, 16). In contrast, induction of CD40L was normal in the previously reported cases of human ICOS deficiency (33). Up-regulation of 4-1BB (CD137), BTLA (CD272), and CTLA-4 (CD152) was normal in ICOS knockout mice (23), as was that of OX40 (CD134) and CTLA-4 in patients with ICOS deficiency in a previous study (31).

We estimated the expression of these costimulatory and inhibitory receptors on ICOS$^{-/-}$ T cells. PBMCs from controls and patients were stimulated with PMA/ionophore (data not shown) or anti-CD3/